Flying under the radar: The non-canonical biochemistry and molecular biology of petrobactin from *Bacillus anthracis*

A.K. Hagan[1], P.E. Carlson Jr.[2], and P.C. Hanna*[1]

1. Department of Microbiology and Immunology, University of Michigan Medical School, 1150 W. Medical Center Drive, 6703 Medical Science Building II, Ann Arbor, MI 48109, Office: (734)615-3706, Fax: (734)764-3562, email: pchanna@umich.edu

2. Laboratory of Mucosal Pathogens and Cellular Immunity, US Food and Drug Administration, Center for Biologics Evaluation and Research, Office of Vaccines Research and Review, Division of Bacterial, Parasitic, and Allergenic Products, 10903 New Hampshire Avenue, Building 52/72; Rm 3306, Silver Spring, MD 20993, Office: (240) 402-4090, Lab: (240) 402-7028, email: paul.carlson@fda.hhs.gov

Keywords: petrobactin, siderophore, *Bacillus anthracis*, regulation, iron, anthrax, pathogenesis

Summary: The dramatic, rapid growth of *Bacillus anthracis* that occurs during systemic anthrax implies a crucial requirement for the efficient acquisition of iron. While recent advances in our understanding of *B. anthracis* iron acquisition systems indicate the use of strategies similar to other pathogens, this review focuses on unique features of the major siderophore system, petrobactin. Ways that petrobactin differs from other siderophores include: A. unique structural elements that allow petrobactin to evade host immune proteins; B. a biosynthetic operon that encodes enzymes from both major siderophore biosynthesis classes; C. redundancy in membrane transport systems for acquisition of Fe-petrobactin holo-complexes; and, D. regulation that appears to be controlled predominately by sensing the host-like environmental signals of temperature, CO_2 levels and oxidative stress, as opposed to canonical sensing of intracellular iron levels. We argue that these differences contribute in meaningful ways to *B. anthracis* pathogenesis. This review will also outline current major gaps in our understanding of the petrobactin iron acquisition system, some projected means for exploiting current knowledge, and potential future research directions.

Introduction:

Iron is the fourth most abundant element on earth and almost all living organisms require iron's redox properties for life. However, these same properties can be toxic for cells, necessitating biological solutions to balance acquisition with stringent regulation(Wandersman and Delepelaire, 2004; Miethke and Marahiel, 2007). The roles of iron as an enzyme cofactor and in electron transfer are a double-edged sword. High, unregulated quantities of iron in the cell are toxic due to the Fenton reaction in which oxidation of ferrous iron generates superoxide radicals resulting in DNA damage(Wandersman and Delepelaire, 2004; Miethke and Marahiel, 2007). Accordingly, iron is tightly regulated at both the cellular and organismal level(Ganz, 2013). Within humans, several proteins are dedicated to iron storage, transfer, and collection: e.g., ferritin, transferrin and lactoferrin, respectively(Finkelstein *et al.*, 1983; Ganz, 2013). Maintaining free ferric iron at less than 10^{-18} μM prevents iron toxicity and easy acquisition by invading bacterial or parasitic pathogens that require iron for growth(Finkelstein *et al.*, 1983; Miethke and Marahiel, 2007; Braun and Hantke, 2011).

Bacillus anthracis is one pathogen that requires iron for growth within a host. The causative agent of anthrax, *B. anthracis* is a Gram-positive, spore-forming bacillus(Dixon *et al.*, 1999; Cote *et al.*, 2011). The metabolically inactive spore is the infectious particle, initiating disease after exposure to an open wound, the respiratory tract, the gastrointestinal tract, or by subcutaneous injection(Dixon *et al.*, 1999; Cote *et al.*, 2011). Preceding systemic anthrax, the spores are engulfed by phagocytes, which migrate to nearby lymph nodes(Dixon *et al.*, 1999). Simultaneous to this migration, spores germinate within the macrophage leading to outgrowth of vegetative cells(Dixon *et al.*, 1999). The vegetative bacilli replicate and produce capsule and toxins, resulting in phagocyte destruction and direct release of bacilli into the lymph or blood(Dixon *et al.*, 1999; Cote *et al.*, 2011). There, they quickly replicate to titers in

excess of 10^8 CFU/mL, preceding death of the host(Cote *et al.*, 2011). This rapid replication requires access to many important nutrients, including iron.

B. anthracis possesses two known mechanisms for acquisition of ferric iron in addition to others for acquisition of ferrous iron (*e.g*. heme)(Carlson *et al.*, 2013). The ferric iron acquisition systems employ iron scavengers known as siderophores(Carlson *et al.*, 2013). During low iron stress, these small molecules are synthesized and transported into the extracellular host milieu to bind ferric iron with a high affinity(Miethke, 2013). The iron-bound (holo) siderophores are then reacquired by the bacterium via a specific receptor allowing iron acquisition and thus sustained growth(Miethke, 2013). *B. anthracis* encodes the biosynthetic machinery for two distinct siderophores, bacillibactin (BB) and petrobactin (PB)(Carlson *et al.*, 2013).

Of the ferric iron acquisition methods, only the siderophore PB is necessary for virulence in murine models of anthrax(Cendrowski *et al.*, 2004; Carlson *et al.*, 2009). Cendrowski, *et al.*, first observed the importance of PB for *B. anthracis* growth when deletion of the anthrax siderophore biosynthetic operon, *asbABCDEF*, led to defects in growth within macrophages *in vitro* and attenuation in spore-challenged mice(Cendrowski *et al.*, 2004). In contrast, strains deficient in BB biosynthesis fail to demonstrate similar growth or virulence defects in either *in vitro* or *in vivo* experiments(Cendrowski *et al.*, 2004; Carlson *et al.*, 2009). It is interesting that while BB is a common siderophore among many *Bacillus* spp., PB has only been identified in the *B. cereus sensu lato* group (*B. cereus, B. thuringiensis and B. anthracis*) and the unrelated Gram-negatives *Marinobacter hydrocarbinoclasticus* and *M. aquaeoli*(Barbeau *et al.*, 2002; Koppisch *et al.*, 2008; Homann *et al.*, 2009). Since the discovery of PB relevance to *B. anthracis* pathogenesis, research has been ongoing.

Petrobactin Structure:

Siderophores are generally classified into four groups according to the major iron binding moieties: hydroxamate, catechol, α-hydroxycarboxylate and mixed (i.e. two or more differing moieties)(Miethke and Marahiel, 2007). These coordinating ligands determine the affinity of a siderophore (pM) for its ferric ligand based on their charge densities and deprotonation values(Miethke and Marahiel, 2007). PB is composed of a citrate backbone with two spermidine arms, each capped by a 3,4-dihydroxybenzoate (3,4-DHB) moiety (Figure 1C) (Barbeau *et al.*, 2002; Gardner *et al.*, 2004). A single ferric iron atom is coordinated between the catechol groups of 3,4-DHB and the α-hydroxycarboxylate of the citrate backbone indicating classification as a mixed type siderophore(Barbeau *et al.*, 2002; Hider and Kong, 2010). Interestingly, PB is the sole siderophore known to use 3,4-DHB instead of the canonical 2,3 configuration. This structural feature coordinates iron with α-hydroxycarboxylate resulting in a lower stability constant of 23pM(Zhang *et al.*, 2009). In contrast, siderophores with three 2,3-DHB moieties (e.g., BB) have stability constants of about 49pM(Zhang *et al.*, 2009; Hider and Kong, 2010)

Petrobactin Biosynthesis:

Siderophores are synthesized by enzymes belonging to either of two families found within operons, the non-ribosomal peptide synthetases (NRPS) or the independent of NRPS synthetases (NIS)(Miethke and Marahiel, 2007; Saha *et al.*, 2013). PB biosynthesis is unique, however, in that both NRPS and NIS enzymes are required. NRPS enzymes are large, multi-enzyme complexes acting in an assembly line fashion to condense a target amino acid into a polypeptide chain(Saha *et al.*, 2013). This machinery has three main domains: the adenylation domain, which activates and recognizes the amino acid, the peptidyl carrier protein (PCP) domain containing a thiolation site and the condensation domain that incorporates the amino acid into the chain(Saha *et al.*, 2013). After the appropriate number of condensation reactions, the peptide is cyclized by a C-terminal thioesterase domain(Saha *et al.*, 2013).

NIS systems, however, are characterized by the presence of ATP-dependent synthetases divided into three functional types, with one split further based on phylogenetics(Oves-Costales *et al.*, 2009). Type A synthetases condense citric acid with either amines or alcohols(Oves-Costales *et al.*, 2009). Type B uses α-ketogluterate as a substrate for condensation with amines, the subgroup type A' acts on citric acid(Oves-Costales *et al.*, 2009). Lastly, type C synthetases condense citric acid or succinic acid derivatives with an amine or alcohol(Oves-Costales *et al.*, 2009). These can also capable oligomerize or macrocycilize σ-amino-carboxylic acids containing a hydroxamate group(Oves-Costales *et al.*, 2009). NIS synthetases can be either "modular", participating in a single condensation reaction or "iterative" participating in two or more condensations with similar substrates(Oves-Costales *et al.*, 2009). This difference cannot be distinguished by sequence comparison analysis(Oves-Costales *et al.*, 2009).

The *asbABCDEF* operon encodes for six enzymes: two belonging to the NIS family (*asbAB*), three NRPS enzymes (*asbCDE*) and one dehydroshikimate dehydratase (*asbF*)(Cendrowski *et al.*, 2004; Oves-Costales *et al.*, 2007; Lee *et al.*, 2007; David T Fox *et al.*, 2008; Pfleger *et al.*, 2008). Briefly, the biosynthetic pathway of PB (Figure 1) begins when AsbF generates 3,4-DHB, which is transferred by AsbC to AsbD. AsbE condenses the 3,4-DHB moiety from AsbD to a molecule of spermidine(David T Fox *et al.*, 2008; Pfleger *et al.*, 2008). Spermidine and citric acid condensation is mediated by AsbA and AsbB to generate multiple intermediates, with the potential for the second 3,4-DHB condensation to occur at multiple points.

The discovery that 3,4-DHB is generated from 3-dehydroshikimate (DHS) by AsbF was published by two groups, Fox *et al.* and Pfleger *et al.* (Figure 1A)(David T Fox *et al.*, 2008; Pfleger *et al.*, 2008). This is the first dehydroshikimate dehydratase (DHSase) to be identified as participating in a non-catabolic pathway(David T. Fox *et al.*, 2008; Pfleger *et al.*, 2008). As predicted by an observed TIM barrel-like fold, AsbF requires divalent cation cofactors with a preference for Mn^{2+} (David T Fox *et al.*, 2008; Pfleger *et al.*, 2008). Structural analysis of AsbF (originally with both cofactor and the product) shows the N-

terminus (Figure 2, blue) partially buried at the bottom of the eight stranded TIM-like barrel (Figure 2, green)(Pfleger *et al.*, 2008). The C-terminus (Figure 2, arrow) is partially solvent exposed. The Mn^{2+} is coordinated by three carboxylic acid side chains (Figure 2B, black), a deprotonated imine (Figure 2B, black) and the 3-hydroxy group of 3,4-DHB (not shown)(Pfleger *et al.*, 2008). In addition to coordinating with Mn^{2+}, 3,4-DHB was bound in the active site by aromatic residues (Figure 2B, red) found under a helical loop (Figure 2, yellow) between the β7 strand and α7 helix(Pfleger *et al.*, 2008). The mechanism of 3,4-DHB generation is predicted to occur in two steps, the generation of an enolate intermediate from 3-DHS, followed by a dehydration step resulting in aromatization and 3,4-DHB product(Pfleger *et al.*, 2008).

Similar to biosynthesis of NRPS siderophores, the aryl product (3,4-DHB) is transferred to a carrier protein (AsbD) by an aryl transferase (AsbC) (Figure 1A-B)(Lee *et al.*, 2007; Pfleger *et al.*, 2007). *In vitro*, AsbC adenylates 3,4-DHB and subsequently loads the substrate, 3,4-DHB-AMP, onto holo-AsbD. Interestingly, this enzyme is highly specific to 3,4-DHB. *In vitro* substitution with 2,3-DHB or 2-hydroxybenzoate, two common aryl acids in siderophores, did not result in substrate adenylation or loading of AsbD(Pfleger *et al.*, 2007). Carrier proteins, such as AsbD, are activated post-translationally by the addition of phosphopantetheine from coenzyme A to a conserved serine (S40 for AsbD)(Pfleger *et al.*, 2007). This reaction is typically catalyzed by a cognate phosphopantethineiyl transferase (PPTase) encoded within the same gene cluster as the carrier protein. There is no PPTase encoded by the *asb* operon, but Pfleger *et al.* predicted AsbD activation *in vivo* by a *B. subtilis sfp* homologue(Pfleger *et al.*, 2007). *E. coli* PPTases were sufficient for AsbD activation *in vitro*, indicating a dedicated PPTase may not be necessary(Pfleger *et al.*, 2007). After generation of 3,4-DHB-loaded AsbD, AsbE catalyzes the condensation of 3,4-DHB to spermidine(Pfleger *et al.*, 2007). Two isomers are generated both *in vitro* and *in vivo* though only the isomer from condensation of 3,4-DHB to the N1 site appears to be incorporated (Figure 1A)(Lee *et al.*, 2007; Pfleger *et al.*, 2007).

AsbA and AsbB are both members of the NIS synthetase family involved in condensation of the citrate backbone to spermidine (Figure 1B)(Oves-Costales *et al.*, 2007; Oves-Costales *et al.*, 2008; Nusca *et al.*, 2012). AsbA is a type A synthetase responsible for the ATP-dependent condensation of citric acid to the N8 site of spermidine(Oves-Costales *et al.*, 2007). Conversely, AsbB is a type C synthetase, catalyzing the condensation of a citrate derivative (in this case N8-citryl-spermidine or 3,4-DHB-citryl-spermidine) with the N8 of a second spermidine molecule(Oves-Costales *et al.*, 2008; Nusca *et al.*, 2012). Condensation of the citrate derivative with 3,4-DHB-spermidine is possible, though not preferred, according to AMP formation rates, suggesting it is unlikely to be a "significant intermediate" in PB biosynthesis(Oves-Costales *et al.*, 2008). Both AsbA and AsbB have similar catalytic activity with similar substrate preferences but are not entirely redundant. In-frame deletion of AsbA does not completely abrogate PB biosynthesis as AsbB functionally compensates for the citrate spermidine condensation *in vitro*. AsbA, however, does not compensate for the loss of AsbB. Indeed, mutants for AsbB fail to produce PB and exhibit reduced growth in iron deficient media(Lee *et al.*, 2007; Oves-Costales *et al.*, 2008; Nusca *et al.*, 2012).

The structure of AsbB resembles a "cupped hand" with three domains: the thumb, palm and fingers (Figure 3 yellow, blue and green, respectively)(Nusca *et al.*, 2012). The active site is composed of basic residues in the finger domain (Figure 3A, red) for the predicted binding of ATP/ADP and acidic residues (Figure 3A, black) responsible for recruitment and stabilization of spermidine in the palm domain(Nusca *et al.*, 2012). Both AsbA and AsbB regioselectively condense citrate to the N8 terminus of spermidine(Nusca *et al.*, 2012). Nusca, *et al.* used site-directed mutagenesis to determine that the charged residues K311 (Figure 3A, purple) and E459 of AsbB (K315/Q468 of AsbA) play roles in determining selectivity for isomer and polyamine incorporation(Nusca *et al.*, 2012). Crystal structure and size exclusion chromatography analyses suggest dimerization of AsbB *in vivo* (Figure 3B) with the pockets containing the active sites connected by a solvent exposed channel. The dimer interaction is

facilitated by the helices Tα1, Tα2, and Tα4 in the thumb domain of one protein with a helix spanning Fα3 and Fα4 of the finger domain of the second(Nusca *et al.*, 2012).

Some questions remain regarding PB biosynthesis. For example, it has not been determined whether the unique biosynthetic process involving both NRPS and NIS synthetases, plus a DHSase occurs in the context of a multi-enzyme or otherwise. There is data to suggest dimerization of AsbB *in vivo*, and the formation of a complex by AsbCDE but nothing to determine if AsbA and/or AsbB interact in vivo with the AsbCDE complex or AsbF(Nusca *et al.*, 2012).

Regulation of Petrobactin Biosynthesis:

For many ferric iron acquisition systems, the ferric uptake regulator (Fur), or a Fur-like protein, is responsible for negative transcriptional regulation of all aspects of the system, including biosynthesis, transport and iron removal. Fur is a negative regulator activated by binding two iron atoms(Wandersman and Delepelaire, 2004). This allows Fur to interact with, and bind, consensus Fur-box sequences upstream of negatively regulated genes. Under iron limiting conditions, the intracellular concentration of iron is reduced such that iron is no longer available to bind Fur(Wandersman and Delepelaire, 2004). Instead, it is used in cellular functions, blocking Fur activation and relieving its transcriptional repression(Wandersman and Delepelaire, 2004).

In *B. anthracis*, Fur inhibits BB biosynthesis(Cendrowski *et al.*, 2004; Hotta *et al.*, 2010). This is less clear with regards to PB regulation. A review by Hotta, *et al.* indicates that the PB biosynthesis operon does not have a conserved upstream Fur-box. Our analysis of the upstream sequences, however, reveals predicted Fur-boxes upstream of both the *asbA* start codon and *fpuAB* (PB receptor and permease, respectively)(Sierro *et al.*, 2008; Hotta *et al.*, 2010). The *fatDCE* operon encoding PB import proteins (Figure 3) also maintains the Fur-box consensus sequence(Hotta *et al.*, 2010). This is contrary to observed microarray data of *B. anthracis* Sterne grown in iron limiting medium where *asbABCDEF* and

fpuAB transcript levels were not significantly altered, but *fatDCE* was significantly induced(Carlson *et al.*, 2009; Carlson *et al.*, 2015). Investigation of BB and PB regulation by Lee *et al.* found that increasing iron concentration decreased supernatant levels of PB, corresponding with changes in transcript levels as measured by qRT-PCR(Lee *et al.*, 2011). However, *asbABCDEF* transcripts were detected in all tested media while BB biosynthesis transcripts (*dhb* operon) were completely abrogated in high iron conditions and rich media(Lee *et al.*, 2011). It is possible that the predicted Fur binding sites for *fpuAB* and *asbABCDEF* are weak allowing for partial, but not complete, regulation of biosynthesis by iron.

In addition to cytoplasmic levels of iron, oxidative stress appears to play a role in PB regulation and biosynthesis. Increases in oxidative stress, due to high aeration or the addition of paraquat, stimulate a dose dependent accumulation of PB in the supernatant(Lee *et al.*, 2011). Accordingly, *asb* transcripts are upregulated during exposure to high aeration, paraquat, or hydrogen peroxide, regardless of iron levels(Lee *et al.*, 2011; Pohl *et al.*, 2011). This pattern differs from that of Fur and Fur-regulated operons, such as BB biosynthesis, which are upregulated only in response to paraquat(Lee *et al.*, 2011; Pohl *et al.*, 2011). Iron import may aid in the oxidative stress response, as paraquat doubles the amount of iron associated with the cell in only sixty minutes(Tu *et al.*, 2012). In the context of a deficient oxidative response (*i.e.* Δ*sodA1*), however, B. anthracis shows a decrease in supernatant PB levels with paraquat addition(Passalacqua *et al.*, 2007; Lee *et al.*, 2011). Lee *et al.* predicted this was due to the sensitivity of PB biosynthetic machinery to oxidative stress(Lee *et al.*, 2011).

Siderophore biosynthesis in *B. anthracis* is also linked to temperature. PB is detected in the supernatant under all conditions tested, with amounts increasing at 30°C and at 37°C while BB production is decreased above 30°C and completely abrogated at 37°C (Garner *et al.*, 2004; Koppisch *et al.*, 2005). Lastly, Wilson *et al.* observed that PB production is increased (and BB decreased) when *B. anthracis* is grown in the presence of 5% CO_2, an atmosphere encountered during growth in the host(Wilson *et al.*, 2010). We note that the environmental conditions resulting in maximal PB

biosynthesis (oxidative stress, 37°C and 5% CO_2) correspond with those expected to be present in the context of a mammalian host.

While many factors (iron concentration, oxidative stress, temperature, and atmosphere) affect PB production, the full mechanism remains undefined. Transcript levels between high and low iron conditions do not appear to vary greatly, but supernatant levels of PB do(Carlson *et al.*, 2009; Lee *et al.*, 2011). This indicates one or more complex mechanisms of post-transcriptional or post-translational regulation of PB biosynthesis. Since PB deficit mutant spores germinate but are unable to outgrow in IDM or macrophages, it is possible the constitutive expression of low levels of PB allow for inclusion into the spore body(Cendrowski *et al.*, 2004; Carlson *et al.*, 2010). Thus, rapid germination can occur inside the iron limiting host environment.

Petrobactin Transport Across Membranes:

Siderophore import requires a dedicated receptor, triggering uptake by specific import machinery(Miethke and Marahiel, 2007). An ATP-binding cassette (ABC) transporter mediates PB import(Dixon *et al.*, 2012). This importer consists of the surface receptor, FpuA (Figure 3, orange) that associates with multiple, specific permeases and ATPases to form three distinct ABC transporters(Carlson *et al.*, 2010; Dixon *et al.*, 2012). These are composed of combinations of the two permeases, FpuB and FatCD (Figure 3, blue), and three ATPases: FpuC, FpuD and FatE (Figure 3, green)(Dixon *et al.*, 2012). Interestingly, either the FpuC or FpuD ATPase can provide energy for the FpuB permease based transporter, while the FatCD permease can only function with the FatE ATPase(Dixon *et al.*, 2012). Inability to import PB leads to a severe growth defect in iron-depleted media, similar to PB biosynthetic mutants, and accumulation of PB in the supernatant[28,29]. These mutants are also severely attenuated in a mouse model of inhalational anthrax, the LD_{50} of *ΔfpuA* is 3-logs greater than wild-type *B. anthracis*(Carlson *et al.*, 2010). While the proteins involved in PB import

are identified, questions remain about how those proteins interact *in vivo* and the molecular mechanisms of PB import.

While PB import has been characterized, the mechanism of apo-PB export following biosynthesis (or iron removal by reduction, if it occurs) in *B. anthracis* is unknown (Figure 3, red). Similar to import, siderophore export occurs via dedicated transporters, the type of transporter family employed varies by siderophore and pathogen, however(Miethke and Marahiel, 2007). We hypothesize from sequence data that PB export from *Marinobacter* spp. occurs from multidrug and toxic compound extrusion (MATE) family transporters located adjacent to the biosynthesis operon. In addition to the MATE family, other types of inner membrane transport proteins, including the resistance nodulation and cell division (RND), major facilitator superfamily (MFS) and ABC transport families, are responsible for export of siderophores in other organisms(Miethke and Marahiel, 2007). Hydroxamate siderophores, such as achromobactin and vibrioferrin, are exported via MFS exporters(Miethke and Marahiel, 2007). In contrast, pyoverdine, a hydroxamate/catechol mixed siderophore, is exported to the periplasm by an ABC-type transporter(Yeterian, Martin, Guillon, *et al.*, 2010). It is difficult to hypothesize which transporter family a PB exporter would belong to due to the unique structure and charge properties of different siderophores.

Iron Release from Petrobactin:

There are two possible fates for enzymatic removal of iron from the siderophore, metal reduction or siderophore hydrolysis. The mechanism for iron removal from PB is unclear, but probably occurs by one of these two mechanisms (Figure 4, gray). Enzymatic hydrolysis of the siderophore backbone in the cytoplasm precedes enzymatic reduction of the iron for incorporation into cellular components. This method is required for siderophores with very high affinities for ferric iron and has been demonstrated in siderophores containing a triacelatone backbone such as enterobactin and

salmochelin[30,32]. In these cases, cleavage occurs at ester sites located on the backbone, requiring specific action by esterases including Fes, IroD and IroE(Langman *et al.*, 1972; Miethke and Marahiel, 2007). Although PB lacks an ester site, cleavage could occur by aminohydrolysis at the citrate/spermidine junctions.

Enzymatic reduction of the iron to its ferrous state lessens the affinity of the siderophore for the substrate. This allows the siderophore to remain intact during iron removal and be recycled extracellularly(Miethke and Marahiel, 2007). This has been demonstrated in siderophores with ferric stability constants less than 30pM, e.g. reduction of ferric-ferrioxamine B by FhuF in *E. coli*(Müller *et al.*, 1998). As the stability constant of PB is 23pM and hydrolysis of amides is more difficult (thus costlier) than ester hydrolysis, we hypothesize iron removal from PB via reduction, not hydrolysis. Central to addressing the question is understanding whether or not PB is fully imported into the cell for iron removal. In the case of *Pseudomonas aeruginosa*, pyoverdin is only imported as far as the periplasm where it undergoes reduction for removal of the iron and is re-exported from the cell(Yeterian, Martin, Lamont, *et al.*, 2010). It is possible ferric-PB is reduced by an unknown enzyme after capture by FpuA then released back to the extracellular milieu for re-use. The identified ABC transporters would be responsible for importing the iron. That seems unlikely, however, for a few reasons. First, it would be more efficient to use the ferrous iron transporter, FeoB, than dedicated permeases. Second, growth of *B. anthracis* in the presence of non-reducible gallium negatively impacts growth. This requires transport of gallium into the cell by PB, thus implying full import of PB-Fe. Third, there is no evidence for this mechanism in Gram-positives(Carlson *et al.*, 2010; Dixon *et al.*, 2012).

Petrobactin and Pathogenesis:

PB is the only method of iron acquisition required for full virulence in a murine model of inhalational anthrax(Cendrowski *et al.*, 2004). Indeed, PB null strains, whether driven by lack of

biosynthesis (*ΔasbABCDEF*) or import (Δ*fpuA*), exhibit a two to three log decrease in LD_{50}(Cendrowski *et al.*, 2004; Carlson *et al.*, 2010). Mutants defective in BB or heme utilization demonstrate little to no effect on virulence(Cendrowski *et al.*, 2004; Gat *et al.*, 2008; Carlson *et al.*, 2009). What makes PB more relevant to *B. anthracis* pathogenesis? We attribute it to regulation and the unique structural features enabling avoidance of the innate immune response and increased iron acquisition.

Studies of PB regulation indicate that conditions relevant to host physiology (5% CO_2 and 37°C) increase PB production but decrease BB production(Garner *et al.*, 2004; Koppisch *et al.*, 2005; Wilson *et al.*, 2010). The differences in PB and BB regulation reflect what is known about the contribution of PB to iron acquisition in the mammalian host over BB. In addition to iron sequestration, neutrophils produce a protein known as siderocalin or lipocalin(Abergel, Clifton, *et al.*, 2008). Siderocalin directly interferes with pathogen iron acquisition by binding siderophores(Abergel, Clifton, *et al.*, 2008). It is capable of binding to ferric-enterobactin and ferric-BB but not glycosylated enterobactin (salmochelin), as glycosylation makes it too large for the binding pocket(Abergel *et al.*, 2006). Ferric-PB is the correct size and charge to be bound by siderocalin(Abergel *et al.*, 2006). However, siderocalin did not recognize PB in *in vitro* studies leading to it's designation as the anthrax "stealth siderophore"(Abergel *et al.*, 2006). Abergel, *et. al.* predicted the orientation of the 3,4-DHB moieties creates a steric hindrance, thus preventing interaction with the rigid binding pocket of siderocalin(Abergel *et al.*, 2006). Another interesting feature of the 3,4-DHB moieties is that they appear to improve sequestration of ferric iron away from transferrin(Abergel, Zawadzka, *et al.*, 2008). While enterobactin has a higher overall affinity for ferric iron, PB removes Fe^{3+} from transferrin up to 6 times more rapidly than enterobactin and 100 times more quickly than the hydroxamate aerobactin(Abergel, Zawadzka, *et al.*, 2008). The authors hypothesized the 3,4-DHB moieties were responsible for this phenomenon. The catechol moieties improve affinity for iron over hydroxamates, hence the increased rate compared to aerobactin(Abergel, Zawadzka, *et al.*, 2008). Since the overall affinity of PB is still lower than enterobactin, perhaps the

unique orientation of the hydroxyl groups provide an increased rate of transfer(Abergel, Zawadzka, *et al.*, 2008). Avoiding sequestration by siderocalin, and thus detection of the innate immune response, together with an increased ability to retrieve ferric iron from transferrin help account for PB's relevance in *B. anthracis* pathogenesis.

A Target for Antibiotics?:

The unique structure of PB confers multiple advantages within the mammalian host environment, and this along with the patterns of regulation, support extrapolation of murine data to the human host. As is the case with other siderophore-producing pathogens, such as *Mycobacterium tuberculosis*, this implies PB use (inclusive of biosynthesis, transport and iron removal) is a viable target for rational anti-*anthracis* drug design(Ferreras *et al.*, 2005). To date, two studies have reported the generation or identification of small molecules targeting PB biosynthetic machinery. First, a rationally-designed acylsulfate analogue of 3,4-DHB-AMP can compete for 3,4-DHB binding to AsbC with submicro-molar affinities(Pfleger *et al.*, 2007). More recently, two small molecules termed baulamycin A and baulamycin B, were found to be potent inhibitors of AsbA activity *in vitro* and of *B. anthracis* growth in both IDM and IRM(Tripathi *et al.*, 2014). These compounds have yet to be tested in animal models. Regardless, the requirement of PB for virulence warrants further exploration of drugs that inhibit PB use in the quest for production of new antibiotics.

Summary and Future Directions:

This review summarized the current knowledge about PB in the context of the pathogen, *Bacillus anthracis*. Interestingly, recent studies have revealed many features of PB regulation, biosynthesis, structure and transport that are unusual, or even unique, in the field of bacterial siderophores. Together, these features enable *B. anthracis* to produce a siderophore under relevant host conditions, that not only gathers the requisite iron for growth, but efficiently and all while "flying

under the radar" of host innate immunity. However, many gaps remain in the current body of knowledge about PB. These include identification of the mechanisms responsible for apo-PB export, iron-removal from holo-PB and regulation of PB biosynthesis. Future research into PB use by *B. anthracis* should focus on addressing these issues and may reveal other non-canonical methods for siderophore acquisition systems. In addition to broadening the field of siderophore research, understanding the "life cycle" of PB use by *B. anthracis* is key for the continued development of targeted antimicrobial therapies.

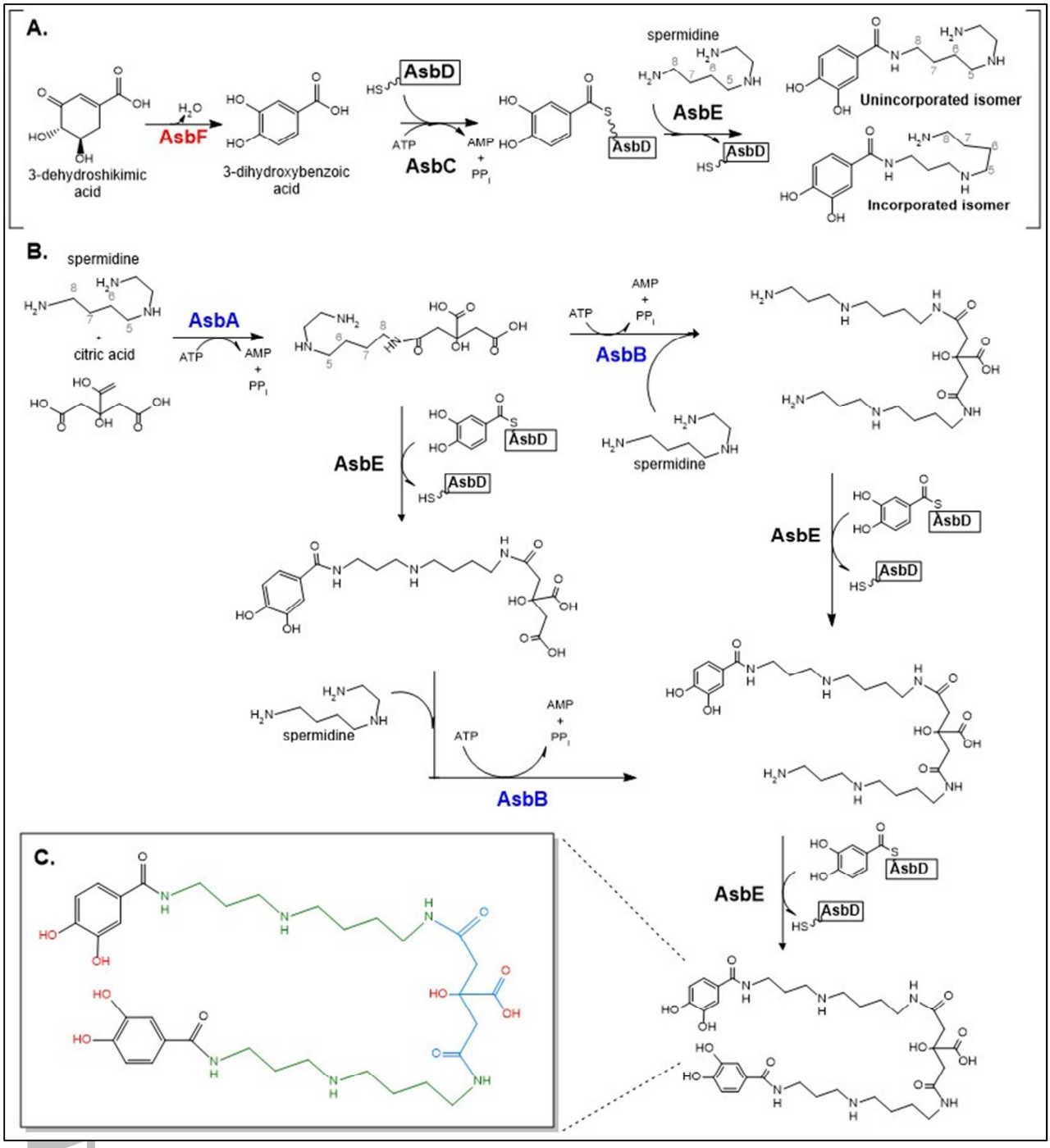

Figure 1. Structure and biosynthesis of petrobactin by Bacillus anthracis. **A**) Following generation of 3,4-DHB by AsbF (red), it is incorporated into petrobactin by three NRPS enzymes, AsbCDE (black text). First it is loaded on to the aryl-carrier protein AsbD by the transferase AsbC. Condensation of 3,4-DHB to a spermidine arm is performed by AsbE. Two isomers are formed, though only the isomer containing 3,4-DHB at the N1-terminus is incorporated into the final product. **B**) NIS enzymes AsbAB (blue text) condense the citrate backbone to spermidine arms. AsbA is efficiently catalyzes the initial reaction of a single spermidine and citrate while AsbB condenses spermidine to a molecule of citryl-spermidine or 3,4-DHB-citryl-spermidine. AsbE and AsbD cap the backbone with 3,4-DHB moieties. **C**) Structure of petrobactin. A citrate backbone (blue) with two spermidine arms (green) each capped with a 3,4-DHB moiety (black). A single molecule of ferric iron is coordinated between each of the 3,4-DHB catechol moieties and the α-hydroxycarboxylate of the citrate backbone (red). Adapted from Nusca, *et. al.*, 2012.

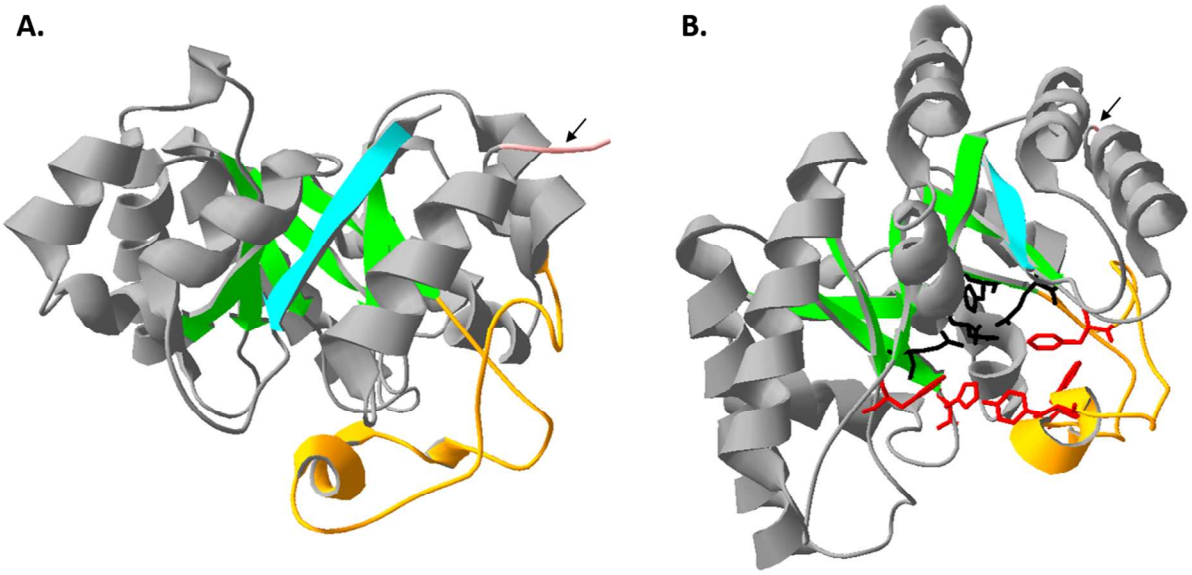

Figure 2. AsbF structure and active site. **A**) Crystal structure of AsbF. The eight β-sheet TIM-barrel (green) occludes the N-terminus (blue) while the C-terminus (salmon, arrow) is exposed. A helical loop (yellow) caps the barrel, closing the active site. **B**) AsbF structure rotated to demonstrate the active site. The Mn2+ is coordinated between residues found within the barrel (black) and 3,4-DHB. In turn, the 3,4-DHB is coordinated by the aromatic residues (red) contributed by helical loops.(Guex and Peitsch, 1997; Pfleger *et al.*, 2008)

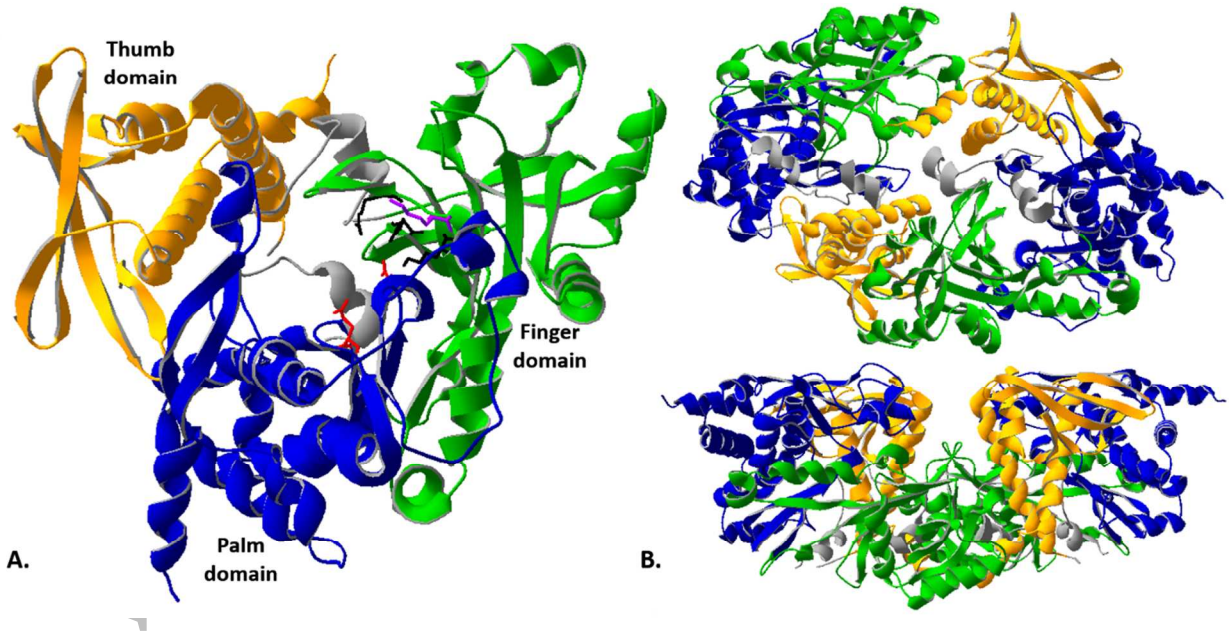

Figure 3. AsbB structure and active site. **A**) Structure and active site of monomeric AsbB. It is composed of three domains; the thumb (yellow), the palm (blue) and the finger (green). The active site is positioned between the palm and finger domains. Basic residues in the palm (red) are predicted to bind ATP/ADP while acidic residues in the finger domain (black, purple) stabilize and selectively recruit spermidine to the active site. **B**) AsbB dimerization is coordinated by the thumb domain (yellow) of one protein with the finger domain (green) of the second (top; view from bottom). This creates a solvent exposed channel (bottom; side view)(Guex and Peitsch, 1997; Nusca *et al.*, 2012).

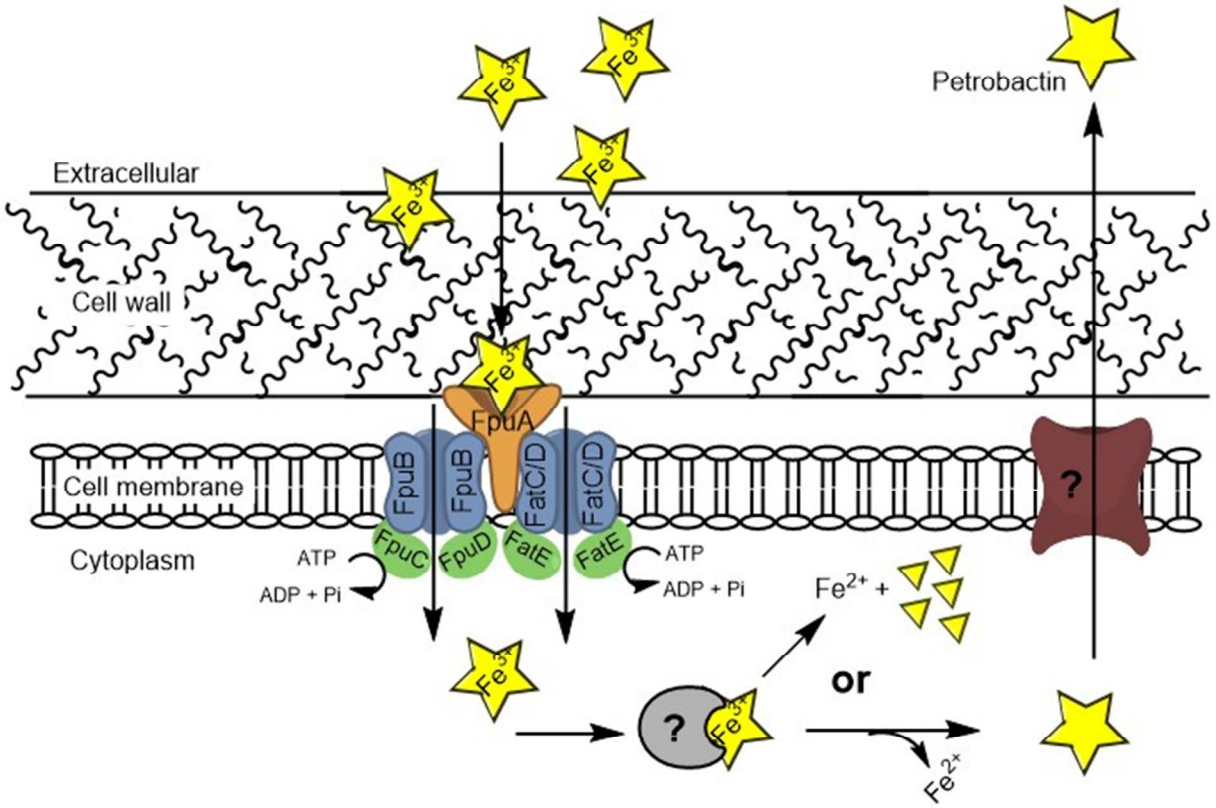

Figure 4. Proposed schematic of petrobactin import, export and iron removal in B. anthracis. Petrobactin (PB, yellow star) is exported via an unknown mechanism. In the supernatant, PB chelates ferric iron and is bound for import by the cell surface recognition protein FpuA (orange). The Fe-PB is then transported by either of two permeases (blue) FpuB or FatCD complexed with an ATPase (green). Energy for transport via FpuB is provided by either FpuC or FpuD while FatCD complexes with the ATPase FatE., The iron is removed from PB by an unknown mechanism (gray) resulting in reduction of iron from intact or hydrolyzed PB.(Carlson *et al.*, 2010; Dixon *et al.*, 2012)

Abergel, R.J., Clifton, M.C., Pizarro, J.C., Warner, J. a, Shuh, D.K., Strong, R.K., and Raymond, K.N. (2008) The siderocalin/enterobactin interaction: a link between mammalian immunity and bacterial iron transport. *J Am Chem Soc* **130**: 11524–34 http://www.pubmedcentral.nih.gov/articlerender.fcgi?artid=3188318&tool=pmcentrez&rendertype=abstract.

Abergel, R.J., Wilson, M.K., Arceneaux, J.E.L., Hoette, T.M., Strong, R.K., Byers, B.R., and Raymond, K.N. (2006) Anthrax pathogen evades the mammalian immune system through stealth siderophore production. *Proc Natl Acad Sci U S A* **103**: 18499–18503 http://www.pubmedcentral.nih.gov/articlerender.fcgi?artid=1693691&tool=pmcentrez&rendertype=abstract.

Abergel, R.J., Zawadzka, A.M., and Raymond, K.N. (2008) Petrobactin-Mediated Iron Transport in Pathogenic Bacteria : Coordination Chemistry of an Unusual 3,4-Catecholate/Citrate Siderophore. *J Am Chem Soc* **130**: 2124–2125.

Barbeau, K., Zhang, G., Live, D.H., and Butler, A. (2002) Petrobactin, a photoreactive siderophore produced by the oil-degrading marine bacterium Marinobacter hydrocarbonoclasticus. *J Am Chem Soc* **124**: 378–9 http://www.ncbi.nlm.nih.gov/pubmed/11792199.

Braun, V., and Hantke, K. (2011) Recent insights into iron import by bacteria. *Curr Opin Chem Biol* **15**: 328–34 http://www.ncbi.nlm.nih.gov/pubmed/21277822. Accessed October 22, 2013.

Carlson, P.E., Bourgis, A.E.T., Hagan, A.K., and Hanna, P.C. (2015) Global gene expression by *Bacillus anthracis* during growth in mammalian blood. *Pathog Dis* **73**: ftv061 http://femspd.oxfordjournals.org/lookup/doi/10.1093/femspd/ftv061.

Carlson, P.E., Carr, K. a, Janes, B.K., Anderson, E.C., and Hanna, P.C. (2009) Transcriptional profiling of Bacillus anthracis Sterne (34F2) during iron starvation. *PLoS One* **4**: e6988 http://www.pubmedcentral.nih.gov/articlerender.fcgi?artid=2742718&tool=pmcentrez&rendertype=abstract. Accessed October 23, 2013.

Carlson, P.E., Dixon, S.D., and Hanna, P.C. (2013) Anthrax and Iron. In *Regulation of Bacterial Virulence*. Vasil, M.L., and Darwin, A.J. (eds). ASM Press, Washington, DC. pp. 307–314.

Carlson, P.E., Dixon, S.D., Janes, B.K., Carr, K. a, Nusca, T.D., Anderson, E.C., *et al.* (2010) Genetic analysis of petrobactin transport in Bacillus anthracis. *Mol Microbiol* **75**: 900–9 http://www.pubmedcentral.nih.gov/articlerender.fcgi?artid=2917102&tool=pmcentrez&rendertype=abstract. Accessed October 21, 2013.

Cendrowski, S., MacArthur, W., and Hanna, P. (2004) Bacillus anthracis requires siderophore biosynthesis for growth in macrophages and mouse virulence. *Mol Microbiol* **51**: 407–17 http://www.ncbi.nlm.nih.gov/pubmed/14756782. Accessed October 23, 2013.

Chazarreta-Cifre, L., Martiarena, L., Mendoza, D. de, and Altabe, S.G. (2011) Role of ferredoxin and flavodoxins in Bacillus subtilis fatty acid desaturation. *J Bacteriol* **193**: 4043–8 http://www.pubmedcentral.nih.gov/articlerender.fcgi?artid=3147679&tool=pmcentrez&rendertype=abstract. Accessed October 23, 2013.

Cote, C.K., Welkos, S.L., and Bozue, J. (2011) Key aspects of the molecular and cellular basis of inhalational anthrax. *Microbes Infect* **13**: 1146–1155 http://www.ncbi.nlm.nih.gov/pubmed/21816231. Accessed October 23, 2013.

Dixon, S.D., Janes, B.K., Bourgis, A., Carlson, P.E., and Hanna, P.C. (2012) Multiple ABC transporters are involved in the acquisition of petrobactin in Bacillus anthracis. *Mol Microbiol* **84**: 370–82

http://www.pubmedcentral.nih.gov/articlerender.fcgi?artid=3323712&tool=pmcentrez&rendertype=abstract. Accessed October 21, 2013.

Dixon, T.C., Meselson, M., Guillemin, J., and Hanna, P.C. (1999) Anthrax. *N Engl J Med* **341**: 815–826.

Ferreras, J. a, Ryu, J.-S., Lello, F. Di, Tan, D.S., and Quadri, L.E.N. (2005) Small-molecule inhibition of siderophore biosynthesis in Mycobacterium tuberculosis and Yersinia pestis. *Nat Chem Biol* **1**: 29–32 http://www.ncbi.nlm.nih.gov/pubmed/16407990. Accessed January 22, 2014.

Finkelstein, R.A., Sciortino, C. V, and McIntosh, M.A. (1983) Role of iron in microbe-host interactions. *Rev Infect Dis* **5 Suppl 4**: S759–S777.

Fox, D.T., Hotta, K., Kim, C., and Koppisch, A.T. (2008) The Missing Link in Petrobactin Biosynthesis : asbF Encodes a (-)-3-Dehydroshikimate Dehydratase. *Biochemistry* **47**: 12251–12253.

Fox, D.T., Hotta, K., Kim, C.Y., and Koppisch, A.T. (2008) The missing link in petrobactin biosynthesis: asbF encodes a (-)-3-dehydroshikimate dehydratase. *Biochemistry* **47**: 12251–12253.

Ganz, T. (2013) Systemic iron homeostasis. *Physiol Rev* **93**: 1721–41 http://www.ncbi.nlm.nih.gov/pubmed/24137020.

Gardner, R.A., Kinkade, R., Wang, C., and Phanstiel, O. (2004) Total synthesis of petrobactin and its homologues as potential growth stimuli for Marinobacter hydrocarbonoclasticus, an oil-degrading bacteria. *J Org Chem* **69**: 3530–7 http://www.ncbi.nlm.nih.gov/pubmed/15132566.

Garner, B.L., Arceneaux, J.E.L., and Byers, B.R. (2004) Temperature control of a 3,4-dihydroxybenzoate (protocatechuate)-based siderophore in Bacillus anthracis. *Curr Microbiol* **49**: 89–94.

Gat, O., Zaide, G., Inbar, I., Grosfeld, H., Chitlaru, T., Levy, H., and Shafferman, A. (2008) Characterization of Bacillus anthracis iron-regulated surface determinant (Isd) proteins containing NEAT domains. *Mol Microbiol* **70**: 983–99 http://www.ncbi.nlm.nih.gov/pubmed/18826411. Accessed January 21, 2014.

Guex, N., and Peitsch, M.C. (1997) SWISS-MODEL and the Swiss-PdbViewer: An environment for comparative protein modeling. *Electrophoresis* **18**: 2714–2723.

Hider, R.C., and Kong, X. (2010) Chemistry and biology of siderophores. *Nat Prod Rep* **27**: 637–57 http://www.ncbi.nlm.nih.gov/pubmed/20376388. Accessed October 23, 2013.

Homann, V. V, Edwards, K.J., Webb, E. a, and Butler, A. (2009) Siderophores of Marinobacter aquaeolei: petrobactin and its sulfonated derivatives. *Biometals* **22**: 565–71 http://www.pubmedcentral.nih.gov/articlerender.fcgi?artid=3066035&tool=pmcentrez&rendertype=abstract. Accessed February 7, 2014.

Hotta, K., Kim, C.-Y., Fox, D.T., and Koppisch, A.T. (2010) Siderophore-mediated iron acquisition in Bacillus anthracis and related strains. *Microbiology* **156**: 1918–25 http://www.ncbi.nlm.nih.gov/pubmed/20466767. Accessed October 23, 2013.

Koppisch, A.T., Browder, C.C., Moe, A.L., Shelley, J.T., Kinkel, B. a, Hersman, L.E., *et al.* (2005) Petrobactin is the primary siderophore synthesized by Bacillus anthracis str. Sterne under conditions of iron starvation. *Biometals* **18**: 577–85 http://www.ncbi.nlm.nih.gov/pubmed/16388397. Accessed October 23, 2013.

Koppisch, A.T., Dhungana, S., Hill, K.K., Boukhalfa, H., Heine, H.S., Colip, L. a, *et al.* (2008) Petrobactin is produced by both pathogenic and non-pathogenic isolates of the Bacillus cereus group of bacteria. *Biometals* **21**: 581–9 http://www.ncbi.nlm.nih.gov/pubmed/18459058. Accessed October 23, 2013.

Langman, L., Young, I.G., Frost, G.E., Rosenberg, H., and Gibson, F. (1972) Enterochelin system of iron transport in Escherichia coli: mutations affecting ferric-enterochelin esterase. *J Bacteriol* **112**: 1142–

1149
http://www.pubmedcentral.nih.gov/articlerender.fcgi?artid=251542&tool=pmcentrez&rendertype=abstract.

Lee, J.Y., Janes, B.K., Passalacqua, K.D., Pfleger, B.F., Bergman, N.H., Liu, H., *et al.* (2007) Biosynthetic analysis of the petrobactin siderophore pathway from Bacillus anthracis. *J Bacteriol* **189**: 1698–710 http://www.pubmedcentral.nih.gov/articlerender.fcgi?artid=1855748&tool=pmcentrez&rendertype=abstract. Accessed October 23, 2013.

Lee, J.Y., Passalacqua, K.D., Hanna, P.C., and Sherman, D.H. (2011) Regulation of petrobactin and bacillibactin biosynthesis in Bacillus anthracis under iron and oxygen variation. *PLoS One* **6**: e20777 http://www.pubmedcentral.nih.gov/articlerender.fcgi?artid=3108971&tool=pmcentrez&rendertype=abstract. Accessed October 23, 2013.

Miethke, M. (2013) Molecular strategies of microbial iron assimilation: from high-affinity complexes to cofactor assembly systems. *Metallomics* **5**: 15–28 http://www.ncbi.nlm.nih.gov/pubmed/23192658. Accessed October 23, 2013.

Miethke, M., and Marahiel, M. a (2007) Siderophore-based iron acquisition and pathogen control. *Microbiol Mol Biol Rev* **71**: 413–451 http://www.pubmedcentral.nih.gov/articlerender.fcgi?artid=2168645&tool=pmcentrez&rendertype=abstract. Accessed January 27, 2014.

Müller, K., Matzanke, B.F., Schünemann, V., Trautwein, a X., and Hantke, K. (1998) FhuF, an iron-regulated protein of Escherichia coli with a new type of [2Fe-2S] center. *Eur J Biochem* **258**: 1001–8 http://www.ncbi.nlm.nih.gov/pubmed/9990318.

Nusca, T.D. (2012) Detailed Analysis of Biosynthetic Components for the Virulence-Associated Siderophore Petrobactin from Bacillus anthracis. .

Nusca, T.D., Kim, Y., Maltseva, N., Lee, J.Y., Eschenfeldt, W., Stols, L., *et al.* (2012) Functional and structural analysis of the siderophore synthetase AsbB through reconstitution of the petrobactin biosynthetic pathway from Bacillus anthracis. *J Biol Chem* **287**: 16058–72 http://www.pubmedcentral.nih.gov/articlerender.fcgi?artid=3346087&tool=pmcentrez&rendertype=abstract. Accessed October 23, 2013.

Oves-Costales, D., Kadi, N., and Challis, G.L. (2009) The long-overlooked enzymology of a nonribosomal peptide synthetase-independent pathway for virulence-conferring siderophore biosynthesis. *Chem Commun (Camb)* 6530–41 http://www.ncbi.nlm.nih.gov/pubmed/19865642. Accessed October 23, 2013.

Oves-Costales, D., Kadi, N., Fogg, M.J., Song, L., Wilson, K.S., and Challis, G.L. (2007) Enzymatic logic of anthrax stealth siderophore biosynthesis: AsbA catalyzes ATP-dependent condensation of citric acid and spermidine. *J Am Chem Soc* **129**: 8416–8417.

Oves-Costales, D., Kadi, N., Fogg, M.J., Song, L., Wilson, K.S., and Challis, G.L. (2008) Petrobactin biosynthesis: AsbB catalyzes condensation of spermidine with N8-citryl-spermidine and its N1-(3,4-dihydroxybenzoyl) derivative. *Chem Commun (Camb)* 4034–6 http://www.ncbi.nlm.nih.gov/pubmed/18758617. Accessed October 23, 2013.

Passalacqua, K.D., Bergman, N.H., Lee, J.Y., Sherman, D.H., and Hanna, P.C. (2007) The global transcriptional responses of Bacillus anthracis Sterne (34F2) and a Delta sodA1 mutant to paraquat reveal metal ion homeostasis imbalances during endogenous superoxide stress. *J Bacteriol* **189**: 3996–4013
http://www.pubmedcentral.nih.gov/articlerender.fcgi?artid=1913413&tool=pmcentrez&rendertype=ab

stract. Accessed October 23, 2013.

Pfleger, B.F., Kim, Y., Nusca, T.D., Maltseva, N., Lee, J.Y., Rath, C.M., *et al.* (2008) Structural and functional analysis of AsbF: origin of the stealth 3,4-dihydroxybenzoic acid subunit for petrobactin biosynthesis. *Proc Natl Acad Sci U S A* **105**: 17133–8 http://www.pubmedcentral.nih.gov/articlerender.fcgi?artid=2579390&tool=pmcentrez&rendertype=abstract.

Pfleger, B.F., Lee, J.Y., Somu, R. V, Aldrich, C.C., Hanna, P.C., and Sherman, D.H. (2007) Characterization and analysis of early enzymes for petrobactin biosynthesis in Bacillus anthracis. *Biochemistry* **46**: 4147–57 http://www.ncbi.nlm.nih.gov/pubmed/17346033.

Pohl, S., Tu, W.Y., Aldridge, P.D., Gillespie, C., Hahne, H., Mäder, U., *et al.* (2011) Combined proteomic and transcriptomic analysis of the response of Bacillus anthracis to oxidative stress. *Proteomics* **11**: 3036–55 http://www.ncbi.nlm.nih.gov/pubmed/21726052. Accessed October 23, 2013.

Saha, R., Saha, N., Donofrio, R.S., and Bestervelt, L.L. (2013) Microbial siderophores: a mini review. *J Basic Microbiol* **53**: 303–17 http://www.ncbi.nlm.nih.gov/pubmed/22733623. Accessed October 23, 2013.

Sierro, N., Makita, Y., Hoon, M. de, and Nakai, K. (2008) DBTBS: a database of transcriptional regulation in Bacillus subtilis containing upstream intergenic conservation information. *Nucleic Acids Res* **36**: D93–6 http://www.pubmedcentral.nih.gov/articlerender.fcgi?artid=2247474&tool=pmcentrez&rendertype=abstract.

Tripathi, A., Schofield, M.M., Chlipala, G.E., Schultz, P.J., Yim, I., Newmister, S.A., *et al.* (2014) Baulamycins A and B, Broad-Spectrum Antibiotics Identified as Inhibitors of Siderophore Biosynthesis in Staphylococcus aureus and Bacillus anthracis. *J Am Chem Soc* **136**: 1579–1586.

Tu, W.Y., Pohl, S., Gray, J., Robinson, N.J., Harwood, C.R., and Waldron, K.J. (2012) Cellular iron distribution in Bacillus anthracis. *J Bacteriol* **194**: 932–40 http://www.pubmedcentral.nih.gov/articlerender.fcgi?artid=3294808&tool=pmcentrez&rendertype=abstract. Accessed October 23, 2013.

Wandersman, C., and Delepelaire, P. (2004) Bacterial iron sources: from siderophores to hemophores. *Annu Rev Microbiol* **58**: 611–47 http://www.ncbi.nlm.nih.gov/pubmed/15487950. Accessed October 23, 2013.

Wilson, M.K., Abergel, R.J., Arceneaux, J.E.L., Raymond, K.N., and Byers, B.R. (2010) Temporal production of the two Bacillus anthracis siderophores, petrobactin and bacillibactin. *Biometals* **23**: 129–34 http://www.pubmedcentral.nih.gov/articlerender.fcgi?artid=3057204&tool=pmcentrez&rendertype=abstract. Accessed October 23, 2013.

Yeterian, E., Martin, L.W., Guillon, L., Journet, L., Lamont, I.L., and Schalk, I.J. (2010) Synthesis of the siderophore pyoverdine in Pseudomonas aeruginosa involves a periplasmic maturation. *Amino Acids* **38**: 1447–59 http://www.ncbi.nlm.nih.gov/pubmed/19787431. Accessed February 18, 2014.

Yeterian, E., Martin, L.W., Lamont, I.L., and Schalk, I.J. (2010) An efflux pump is required for siderophore recycling by Pseudomonas aeruginosa. *Environ Microbiol Rep* **2**: 412–8 http://www.ncbi.nlm.nih.gov/pubmed/23766114. Accessed October 23, 2013.

Zhang, G., Amin, S.A., Küpper, F.C., Holt, P.D., Carrano, C.J., and Butler, A. (2009) Ferric stability constants of representative marine siderophores: marinobactins, aquachelins, and petrobactin. *Inorg Chem* **48**: 11466–73

http://www.pubmedcentral.nih.gov/articlerender.fcgi?artid=2790009&tool=pmcentrez&rendertype=abstract. Accessed October 23, 2013.

Flying under the radar: The non-canonical biochemistry and molecular biology of petrobactin from *Bacillus anthracis*

A.K. Hagan[1], P.E. Carlson Jr.[2], and P.C. Hanna*[1]

1. Department of Microbiology and Immunology, University of Michigan Medical School, 1150 W. Medical Center Drive, 6703 Medical Science Building II, Ann Arbor, MI 48109, Office: (734)615-3706, Fax: (734)764-3562, email: pchanna@umich.edu

2. Laboratory of Mucosal Pathogens and Cellular Immunity, Division of Bacterial, Parasitic, and Allergenic Products, Office of Vaccines Research and Review, Center for Biologics Evaluation and Research, US Food and Drug Administration. 10903 New Hampshire Avenue, Building 52/72; Rm 3306, Silver Spring, MD 20993, Office: (240) 402-4090, email: paul.carlson@fda.hhs.gov

Keywords: petrobactin, siderophore, *Bacillus anthracis*, regulation, iron, anthrax, pathogenesis

Abbreviated Summary: This review aims to discuss the current state of knowledge regarding petrobactin use by the pathogen *Bacillus anthracis*. Used to gather iron during infections, petrobactin differs from other siderophores in a number of ways including: regulation, biosynthesis, structure, and transport. We argue that these differences enhance the pathogenic ability of *B. anthracis* through increased iron acquisition, and identify areas needing further research.

Flying under the radar: The non-canonical biochemistry and molecular biology of petrobactin from *Bacillus anthracis*

A.K. Hagan[1], P.E. Carlson Jr.[2], and P.C. Hanna*[1]

1. Department of Microbiology and Immunology, University of Michigan Medical School, 1150 W. Medical Center Drive, 6703 Medical Science Building II, Ann Arbor, MI 48109, Office: (734)615-3706, Fax: (734)764-3562, email: pchanna@umich.edu

2. Laboratory of Mucosal Pathogens and Cellular Immunity, Division of Bacterial, Parasitic, and Allergenic Products, Office of Vaccines Research and Review, Center for Biologics Evaluation and Research, US Food and Drug Administration. 10903 New Hampshire Avenue, Building 52/72; Rm 3306, Silver Spring, MD 20993, Office: (240) 402-4090, email: paul.carlson@fda.hhs.gov

Keywords: petrobactin, siderophore, *Bacillus anthracis*, regulation, iron, anthrax, pathogenesis

Summary: The dramatic, rapid growth of *Bacillus anthracis* that occurs during systemic anthrax implies a crucial requirement for the efficient acquisition of iron. While recent advances in our understanding of *B. anthracis* iron acquisition systems indicate the use of strategies similar to other pathogens, this review focuses on unique features of the major siderophore system, petrobactin. Ways that petrobactin differs from other siderophores include: A. unique ferric iron binding moieties that allow petrobactin to evade host immune proteins; B. a biosynthetic operon that encodes enzymes from both major siderophore biosynthesis classes; C. redundancy in membrane transport systems for acquisition of Fe-petrobactin holo-complexes; and, D. regulation that appears to be controlled predominately by sensing the host-like environmental signals of temperature, CO_2 levels and oxidative stress, as opposed to canonical sensing of intracellular iron levels. We argue that these differences contribute in meaningful ways to *B. anthracis* pathogenesis. This review will also outline current major gaps in our understanding of the petrobactin iron acquisition system, some projected means for exploiting current knowledge, and potential future research directions.

Introduction:

Iron is the fourth most abundant element on earth and almost all living organisms require iron's redox properties for life. However, these same properties can be toxic for cells, necessitating biological solutions to balance acquisition with stringent regulation(Wandersman and Delepelaire, 2004; Miethke and Marahiel, 2007). The roles of iron as an enzyme cofactor and in electron transfer are a double-edged sword. High, unregulated quantities of iron in the cell are toxic due to the Fenton reaction in which oxidation of ferrous iron generates superoxide radicals resulting in DNA damage(Wandersman and Delepelaire, 2004; Miethke and Marahiel, 2007). Accordingly, iron is tightly regulated at both the cellular and organismal level(Ganz, 2013). Within humans, several proteins are dedicated to iron storage, transfer, and collection: e.g., ferritin, transferrin and lactoferrin, respectively(Finkelstein *et al.*, 1983; Ganz, 2013). Maintaining free ferric iron at less than 10^{-18} μM prevents iron toxicity and easy acquisition by invading bacterial or parasitic pathogens that require iron for growth(Finkelstein *et al.*, 1983; Miethke and Marahiel, 2007; Braun and Hantke, 2011).

Bacillus anthracis is one pathogen that requires iron for growth within a host. The causative agent of anthrax, *B. anthracis* is a Gram-positive, spore-forming bacillus. The metabolically inactive spore is the infectious particle, initiating disease after exposure to an open wound, the respiratory tract, the gastrointestinal tract, or by subcutaneous injection(Dixon *et al.*, 1999; Cote *et al.*, 2011; Palmateer *et al.*, 2013). Preceding systemic anthrax, the spores are engulfed by phagocytes, which migrate to nearby lymph nodes. Simultaneous to this migration, spores germinate within the macrophage or dendritic cell leading to outgrowth of vegetative cells(Ross, 1957; Dixon *et al.*, 1999; Brittingham *et al.*, 2005). The vegetative bacilli replicate and produce toxins, resulting in phagocyte destruction and direct release of bacilli into the lymph or blood(Dixon *et al.*, 1999; Banks *et al.*, 2005; Cote *et al.*, 2011). There, they quickly replicate to titers in excess of 10^8 CFU/mL, preceding death of the host(Lincoln *et al.*, 1967; Friedlander *et al.*, 1993; Cote *et al.*, 2011). This rapid replication requires access to many important nutrients, including iron.

B. anthracis possesses two known mechanisms for acquisition of ferric iron in addition to others for acquisition of ferrous iron (*e.g*. heme)(Carlson *et al.*, 2013). The ferric iron acquisition systems employ iron scavengers known as siderophores. During low iron stress, these small molecules are synthesized and transported into the extracellular host milieu to bind ferric iron with a high affinity(Miethke, 2013). The iron-bound (holo) siderophores are then reacquired by the bacterium via a specific receptor allowing iron acquisition and thus sustained growth(Miethke, 2013). *B. anthracis* encodes the biosynthetic machinery for two distinct siderophores, bacillibactin (BB) and petrobactin (PB)(Cendrowski *et al.*, 2004).

Of the ferric iron acquisition methods, only the siderophore PB is necessary for virulence in murine models of anthrax(Cendrowski *et al.*, 2004; Carlson *et al.*, 2009). Cendrowski, *et al.*, first observed the importance of PB for *B. anthracis* growth when deletion of the anthrax siderophore biosynthetic operon, *asbABCDEF*, led to defects in growth within macrophages *in vitro* and attenuation in spore-challenged mice(Cendrowski *et al.*, 2004). In contrast, strains deficient in BB biosynthesis fail to demonstrate similar growth or virulence defects in either *in vitro* or *in vivo* experiments(Cendrowski *et al.*, 2004; Carlson *et al.*, 2009). It is interesting that while BB is a common siderophore among many *Bacillus* spp., PB biosynthesis has only been identified in the *B. cereus sensu lato* group (*B. cereus, B. thuringiensis and B. anthracis*) and the unrelated Gram-negatives *Marinobacter hydrocarbinoclasticus* and *M. aquaeoli*(Barbeau *et al.*, 2002; Koppisch *et al.*, 2008; Homann *et al.*, 2009). Since the discovery of PB relevance to *B. anthracis* pathogenesis, research has been ongoing.

Petrobactin Structure:

Siderophores are generally classified into four groups according to the major iron binding moieties: hydroxamate, catechol, α-hydroxycarboxylate and mixed (*i.e*. either two or more differing moieties or the use of less common iron binding moieties)(Miethke and Marahiel, 2007). These

coordinating ligands determine the affinity of a siderophore (pM) for its ferric ligand based on their charge densities and deprotonation values and is calculated based on the concentration of free Fe^{3+} remaining at equilibrium (Miethke and Marahiel, 2007; Zhang *et al.*, 2009). PB is composed of a citrate backbone with two spermidine arms, each capped by a 3,4-dihydroxybenzoate (3,4-DHB) moiety (Figure 1C) (Barbeau *et al.*, 2002; Gardner *et al.*, 2004). A single ferric iron atom is coordinated between the catechol groups of 3,4-DHB and the α-hydroxycarboxylate of the citrate backbone, indicating classification as a mixed-type siderophore(Barbeau *et al.*, 2002; Hider and Kong, 2010). Interestingly, PB is the sole siderophore known to use 3,4-DHB instead of the canonical 2,3 configuration. The coordination of ferric iron with these alternate catechol moieties and α-hydroxycarboxylate results in a ferric affinity of 23pM for PB (Zhang *et al.*, 2009). In contrast, siderophores with three 2,3-DHB moieties (e.g., BB) have higher ferric affinities of about 35pM, a 12 log difference(Zhang *et al.*, 2009; Hider and Kong, 2010).

Petrobactin Biosynthesis:

Siderophores are synthesized by enzymes belonging to either of two families found within operons, the non-ribosomal peptide synthetases (NRPS) or the independent of NRPS synthetases (NIS)(Miethke and Marahiel, 2007; Saha *et al.*, 2013). PB biosynthesis is unique, however, in that both NRPS and NIS enzymes are required. NRPS enzymes are large, multi-enzyme complexes acting in an assembly line fashion to condense a target amino acid into a polypeptide chain(Finking and Marahiel, 2004; Saha *et al.*, 2013). This machinery has three main domains: the adenylation domain, which activates and recognizes the amino acid, the peptidyl carrier protein (PCP) domain containing a thiolation site and the condensation domain that incorporates the amino acid into the chain(Conti *et al.*, 1997; Stachelhaus *et al.*, 1999; Keating *et al.*, 2000; Weber *et al.*, 2000; Keating *et al.*, 2002; May *et al.*, 2002; Finking and Marahiel, 2004). After the appropriate number of condensation reactions, the peptide

is cyclized by a C-terminal thioesterase domain(Schneider and Marahiel, 1998; Finking and Marahiel, 2004; Sieber and Marahiel, 2008).

NIS systems, however, are characterized by the presence of ATP-dependent synthetases divided into three functional types, with one split further based on phylogenetics(Challis, 2005). Type A synthetases condense citric acid with either amines or alcohols(Oves-Costales, Kadi, *et al.*, 2009). Type B uses α-ketogluterate as a substrate for condensation with amines, the subgroup type A' acts on citric acid(Oves-Costales, Kadi, *et al.*, 2009). Lastly, type C synthetases condense citric acid or succinic acid derivatives with an amine or alcohol(Kadi *et al.*, 2007; Schmelz *et al.*, 2009; Oves-Costales, Kadi, *et al.*, 2009). These can also oligomerize or macrocycilize σ-amino-carboxylic acids containing a hydroxamate group(Kadi *et al.*, 2007; Oves-Costales, Kadi, *et al.*, 2009). NIS synthetases can be either "modular", participating in a single condensation reaction or "iterative" participating in two or more condensations with similar substrates(Oves-Costales, Kadi, *et al.*, 2009). This difference cannot be distinguished by sequence comparison analysis(Oves-Costales, Kadi, *et al.*, 2009).

The *asbABCDEF* operon encodes for six enzymes: two belonging to the NIS family (*asbAB*), three NRPS enzymes (*asbCDE*) and one dehydroshikimate dehydratase (*asbF*)(Cendrowski *et al.*, 2004; Oves-Costales *et al.*, 2007; Lee *et al.*, 2007; Fox *et al.*, 2008; Pfleger *et al.*, 2008). Briefly, the biosynthetic pathway of PB (Figure 1) begins when AsbF generates 3,4-DHB, which is transferred by AsbC to AsbD. AsbE condenses the 3,4-DHB moiety from AsbD to a molecule of spermidine(Fox *et al.*, 2008; Pfleger *et al.*, 2008). Spermidine and citric acid condensation is mediated by AsbA and AsbB to generate multiple intermediates, with the potential for the second 3,4-DHB condensation to occur at multiple points.

The discovery that 3,4-DHB is generated from 3-dehydroshikimate (DHS) by AsbF was published by two groups, Fox *et al.* and Pfleger *et al.* (Figure 1A)(Fox *et al.*, 2008; Pfleger *et al.*, 2008). This is the first dehydroshikimate dehydratase (DHSase) to be identified as participating in a non-catabolic

pathway(Fox *et al.*, 2008; Pfleger *et al.*, 2008). As predicted by an observed TIM barrel-like fold, AsbF requires divalent cation cofactors with a preference for Mn^{2+} (Fox *et al.*, 2008; Pfleger *et al.*, 2008). Structural analysis of AsbF (originally with both cofactor and the product) shows the N-terminus (Figure 2, blue) partially buried at the bottom of the eight stranded TIM-like barrel (Figure 2, green)(Pfleger *et al.*, 2008). The C-terminus (Figure 2, arrow) is partially solvent exposed. The Mn^{2+} is coordinated by three carboxylic acid side chains (Figure 2B, black), a deprotonated imine (Figure 2B, black) and the 3-hydroxy group of 3,4-DHB (not shown)(Pfleger *et al.*, 2008). In addition to coordinating with Mn^{2+}, 3,4-DHB was bound in the active site by aromatic residues (Figure 2B, red) found under a helical loop (Figure 2, yellow) between the β7 strand and α7 helix(Pfleger *et al.*, 2008). The mechanism of 3,4-DHB generation is predicted to occur in two steps, the generation of an enolate intermediate from 3-DHS, followed by a dehydration step resulting in aromatization and 3,4-DHB product(Pfleger *et al.*, 2008).

Similar to biosynthesis of NRPS siderophores, the aryl product (3,4-DHB) is transferred to a carrier protein (AsbD) by an aryl transferase (AsbC) (Figure 1A-B)(Lee *et al.*, 2007; Pfleger *et al.*, 2007). *In vitro*, AsbC adenylates 3,4-DHB and subsequently loads the substrate, 3,4-DHB-AMP, onto holo-AsbD, the PCP. Interestingly, AsbC is highly specific to 3,4-DHB. *In vitro* substitution with 2,3-DHB or 2-hydroxybenzoate, two common aryl acids in siderophores, did not result in substrate adenylation or loading of AsbD(Pfleger *et al.*, 2007). Carrier proteins, such as AsbD, are activated post-translationally by the addition of phosphopantetheine from coenzyme A to a conserved serine (S40 for AsbD)(Pfleger *et al.*, 2007). This reaction is typically catalyzed by a cognate phosphopantethineiyl transferase (PPTase) encoded within the same gene cluster as the carrier protein. There is no PPTase encoded by the *asb* operon, but Pfleger *et al.* predicted AsbD activation *in vivo* by a *B. subtilis sfp* homologue(Pfleger *et al.*, 2007). *E. coli* PPTases were sufficient for AsbD activation *in vitro*, indicating a dedicated PPTase may not be necessary(Pfleger *et al.*, 2007). After generation of 3,4-DHB-loaded AsbD, AsbE catalyzes the condensation of 3,4-DHB to spermidine(Pfleger *et al.*, 2007). Two isomers are generated both *in vitro*

and *in vivo* though only the isomer from condensation of 3,4-DHB to the N1 site appears to be incorporated (Figure 1A)(Lee *et al.*, 2007; Pfleger *et al.*, 2007).

AsbA and AsbB are both members of the NIS synthetase family involved in condensation of the citrate backbone to spermidine (Figure 1B)(Oves-Costales *et al.*, 2007; Oves-Costales *et al.*, 2008; Nusca *et al.*, 2012). AsbA is a type A synthetase responsible for the ATP-dependent condensation of citric acid to the N8 site of spermidine(Oves-Costales *et al.*, 2007). Biochemical studies indicate AsbA can catalyze condensation reactions with citrate or spermidine analogs through a potentially novel process (Oves-Costales, Song, *et al.*, 2009). Conversely, AsbB is a type C synthetase, catalyzing the condensation of a citrate derivative (in this case N8-citryl-spermidine or 3,4-DHB-citryl-spermidine) with the N8 of a second spermidine molecule(Oves-Costales *et al.*, 2008; Nusca *et al.*, 2012). Condensation of the citrate derivative with 3,4-DHB-spermidine is possible, though not preferred, according to AMP formation rates, suggesting it is unlikely to be a "significant intermediate" in PB biosynthesis(Oves-Costales *et al.*, 2008). Both AsbA and AsbB have similar catalytic activity with similar substrate preferences in regards to PB but are not entirely redundant. In-frame deletion of AsbA does not completely abrogate PB biosynthesis as AsbB functionally compensates for the citrate spermidine condensation *in vitro*. AsbA, however, does not compensate for the loss of AsbB as mutants for AsbB fail to produce PB and exhibit reduced growth in iron deficient media(Lee *et al.*, 2007; Oves-Costales *et al.*, 2008; Nusca *et al.*, 2012).

The structure of AsbB resembles a "cupped hand" with three domains: the thumb, palm and fingers (Figure 3 yellow, blue and green, respectively)(Schmelz *et al.*, 2009; Nusca *et al.*, 2012). The active site is composed of basic residues in the finger domain (Figure 3A, red) for the predicted binding of ATP/ADP and acidic residues (Figure 3A, black) responsible for recruitment and stabilization of spermidine in the palm domain(Nusca *et al.*, 2012). Both AsbA and AsbB regioselectively condense citrate to the N8 terminus of spermidine(Nusca *et al.*, 2012). Nusca, *et al.* used site-directed mutagenesis to determine that the charged residues K311 (Figure 3A, purple) and E459 of AsbB

(K315/Q468 of AsbA) play roles in determining selectivity for isomer and polyamine incorporation(Nusca *et al.*, 2012). Crystal structure and size exclusion chromatography analyses suggest dimerization of AsbB *in vivo* (Figure 3B) with the pockets containing the active sites connected by a solvent exposed channel. The dimer interaction is facilitated by the helices Tα1, Tα2, and Tα4 in the thumb domain of one protein with a helix spanning Fα3 and Fα4 of the finger domain of the second(Nusca *et al.*, 2012).

Some questions remain regarding PB biosynthesis. For example, it has not been determined whether the unique biosynthetic process involving both NRPS and NIS synthetases, plus a DHSase occurs in the context of a multi-enzyme or otherwise. There is data to suggest dimerization of AsbB (and other type C synthetases) *in vivo*, as well as the formation of a complex by AsbCDE, but nothing to determine if AsbA and/or AsbB interact in vivo with the AsbCDE complex or AsbF(Schmelz *et al.*, 2009; Nusca *et al.*, 2012).

Regulation of Petrobactin Biosynthesis:

For many ferric iron acquisition systems, the ferric uptake regulator (Fur), or a Fur-like protein, is responsible for negative transcriptional regulation of all aspects of the system, including biosynthesis, transport and iron removal(Wandersman and Delepelaire, 2004). Fur is a negative regulator activated by binding two iron atoms(Ernst *et al.*, 1978; Hantke, 1981; Bagg and Neilands, 1987). This allows Fur to interact with, and bind, consensus Fur-box sequences upstream of negatively regulated genes(Stojiljkovic *et al.*, 1994; Lavrrar and Mcintosh, 2003). Under iron limiting conditions, the intracellular concentration of iron is reduced such that iron is no longer available to bind Fur. Instead, it is used in cellular functions, blocking Fur activation and relieving its transcriptional repression(Wandersman and Delepelaire, 2004).

In *B. anthracis*, Fur inhibits BB biosynthesis(Cendrowski *et al.*, 2004; Hotta *et al.*, 2010). This is less clear with regards to PB regulation. A review by Hotta, *et al.* indicates that the PB biosynthesis

operon does not have a conserved upstream Fur-box. Our analysis of the upstream sequences, however, reveals predicted Fur-boxes upstream of both the *asbA* start codon and *fpuAB* (PB receptor and permease, respectively)(Sierro *et al.*, 2008; Hotta *et al.*, 2010). The *fatDCE* operon encoding PB import proteins (Figure 3) also maintains the Fur-box consensus sequence(Hotta *et al.*, 2010). This is contrary to observed microarray data of *B. anthracis* Sterne grown in iron limiting medium where *asbABCDEF* and *fpuAB* transcript levels were not significantly altered, but *fatDCE* was significantly induced(Carlson *et al.*, 2009; Carlson *et al.*, 2015). Investigation of BB and PB regulation by Lee *et al.* found that increasing iron concentration decreased supernatant levels of PB, corresponding with changes in transcript levels as measured by qRT-PCR(Lee *et al.*, 2011). However, *asbABCDEF* transcripts were detected in all tested media while BB biosynthesis transcripts (*dhb* operon) were completely abrogated in high iron conditions and rich media(Lee *et al.*, 2011). It is possible that the predicted Fur binding sites for *fpuAB* and *asbABCDEF* are weak allowing for partial, but not complete, regulation of biosynthesis by iron.

In addition to cytoplasmic levels of iron, oxidative stress appears to play a role in PB regulation and biosynthesis. Increases in oxidative stress, due to high aeration or the addition of paraquat, stimulate a dose dependent accumulation of PB in the supernatant(Lee *et al.*, 2011). Accordingly, *asb* transcripts are upregulated during exposure to high aeration, paraquat, or hydrogen peroxide, regardless of iron levels(Lee *et al.*, 2011; Pohl *et al.*, 2011). This pattern differs from that of Fur and Fur-regulated operons, such as BB biosynthesis, which are upregulated only in response to paraquat(Lee *et al.*, 2011; Pohl *et al.*, 2011). Iron import may aid in the oxidative stress response, as paraquat doubles the amount of iron associated with the cell in only sixty minutes(Tu *et al.*, 2012). In the context of a deficient oxidative response (*i.e.* Δ*sodA1*), however, B. anthracis shows a decrease in supernatant PB levels with paraquat addition(Passalacqua *et al.*, 2007; Lee *et al.*, 2011). Lee *et al.* predicted this was due to the sensitivity of PB biosynthetic machinery to oxidative stress(Lee *et al.*, 2011).

Siderophore biosynthesis in *B. anthracis* is also linked to temperature. PB is detected in the supernatant under all conditions tested, with amounts increasing at 30°C and at 37°C while BB production is decreased above 30°C and completely abrogated at 37°C (Garner *et al.*, 2004; Koppisch *et al.*, 2005). Lastly, Wilson *et al.* observed that PB production is increased (and BB decreased) when *B. anthracis* is grown in the presence of 5% CO_2, an atmosphere encountered during growth in the host(Wilson *et al.*, 2010). We note that the environmental conditions resulting in maximal PB biosynthesis (oxidative stress, 37°C and 5% CO_2) correspond with those expected to be present in the context of a mammalian host.

While many factors (iron concentration, oxidative stress, temperature, and atmosphere) affect PB production, the full mechanism remains undefined. Transcript levels between high and low iron conditions do not appear to vary greatly, but supernatant levels of PB do(Carlson *et al.*, 2009; Lee *et al.*, 2011). This indicates one or more complex mechanisms of post-transcriptional or post-translational regulation of PB biosynthesis. Since PB deficit mutant spores germinate but are unable to outgrow in IDM or macrophages, it is possible the constitutive expression of low levels of PB allow for inclusion into the spore body(Cendrowski *et al.*, 2004; Carlson *et al.*, 2010). Thus, rapid germination can occur inside the iron limiting host environment.

Petrobactin Transport Across Membranes:

Siderophore import requires a dedicated receptor, triggering uptake by specific import machinery(Miethke and Marahiel, 2007). An ATP-binding cassette (ABC) transporter mediates PB import(Dixon *et al.*, 2012). This importer consists of the surface receptor, FpuA (Figure 3, orange) that associates with multiple, specific permeases and ATPases to form three distinct ABC transporters(Carlson *et al.*, 2010; Dixon *et al.*, 2012). These are composed of combinations of the two permeases, FpuB and FatCD (Figure 3, blue), and three ATPases: FpuC, FpuD and FatE (Figure 3,

green)(Dixon *et al.*, 2012). Interestingly, either the FpuC or FpuD ATPase can provide energy for the FpuB permease based transporter, while the FatCD permease can only function with the FatE ATPase(Dixon *et al.*, 2012). Inability to import PB leads to a severe growth defect in iron-depleted media, similar to PB biosynthetic mutants, and accumulation of PB in the supernatant[28,29]. These mutants are also severely attenuated in a mouse model of inhalational anthrax, the LD_{50} of *ΔfpuA* is 3-logs greater than wild-type *B. anthracis*(Carlson *et al.*, 2010). While the proteins involved in PB import are identified, questions remain about how those proteins interact *in vivo* and the molecular mechanisms of PB import.

While PB import has been characterized, the mechanism of apo-PB export following biosynthesis (or iron removal by reduction, if it occurs) in *B. anthracis* is unknown (Figure 3, red). Similar to import, siderophore export occurs via dedicated transporters, the type of transporter family employed varies by siderophore and pathogen, however(Miethke and Marahiel, 2007). We hypothesize from sequence data that PB export from *Marinobacter* spp. occurs from multidrug and toxic compound extrusion (MATE) family transporters located adjacent to the biosynthesis operon. In addition to the MATE family, other types of inner membrane transport proteins, including the resistance nodulation and cell division (RND), major facilitator superfamily (MFS) and ABC transport families, are responsible for export of siderophores in other organisms(Miethke and Marahiel, 2007). Hydroxamate siderophores, such as achromobactin and vibrioferrin, are exported via MFS exporters(Miethke and Marahiel, 2007). In contrast, pyoverdine, a hydroxamate/catechol mixed siderophore, is exported to the periplasm by an ABC-type transporter(Yeterian, Martin, Guillon, *et al.*, 2010). It is difficult to hypothesize which transporter family a PB exporter would belong to due to the unique structure and charge properties of different siderophores.

Iron Release from Petrobactin:

There are two possible fates for enzymatic removal of iron from the siderophore, metal reduction or siderophore hydrolysis. The mechanism for iron removal from PB is unclear, but probably occurs by one of these two mechanisms (Figure 4, gray). Enzymatic hydrolysis of the siderophore backbone in the cytoplasm precedes enzymatic reduction of the iron for incorporation into cellular components. This method is required for siderophores with very high affinities for ferric iron and has been demonstrated in siderophores containing a triacelatone backbone such as enterobactin and salmochelin[30,32]. In these cases, cleavage occurs at ester sites located on the backbone, requiring specific action by esterases including Fes, IroD and IroE(Langman *et al.*, 1972; Miethke and Marahiel, 2007). Although PB lacks an ester site, cleavage could occur by amide hydrolysis at the citrate/spermidine junctions.

Enzymatic reduction of the iron to its ferrous state lessens the affinity of the siderophore for the substrate. This allows the siderophore to remain intact during iron removal and be recycled extracellularly(Miethke and Marahiel, 2007). This has been demonstrated in siderophores with ferric stability constants less than 30pM, e.g. reduction of ferric-ferrioxamine B by FhuF in *E. coli*(Müller *et al.*, 1998). As the stability constant of PB is 23pM and hydrolysis of amides is more difficult (thus costlier) than ester hydrolysis, we hypothesize iron removal from PB via reduction, not hydrolysis. Central to addressing the question is understanding whether or not PB is fully imported into the cell for iron removal. In the case of *Pseudomonas aeruginosa*, pyoverdin is only imported as far as the periplasm where it undergoes reduction for removal of the iron and is re-exported from the cell(Yeterian, Martin, Lamont, *et al.*, 2010). It is possible ferric-PB is reduced by an unknown enzyme after capture by FpuA then released back to the extracellular milieu for re-use. The identified ABC transporters would be responsible for importing the iron. That seems unlikely, however, for a few reasons. First, it would be more efficient to use the ferrous iron transporter, FeoB, than dedicated permeases. Second, growth of *B. anthracis* in the presence of non-reducible gallium negatively impacts growth. This requires transport

of gallium into the cell by PB, thus implying full import of PB-Fe. Third, there is no evidence for this mechanism in Gram-positives(Carlson *et al.*, 2010; Dixon *et al.*, 2012).

Petrobactin and Pathogenesis:

PB is the only method of iron acquisition required for full virulence in a murine model of inhalational anthrax(Cendrowski *et al.*, 2004). Indeed, PB null strains, whether driven by lack of biosynthesis (*ΔasbABCDEF*) or import (Δ*fpuA*), exhibit a two to three log decrease in LD_{50}(Cendrowski *et al.*, 2004; Carlson *et al.*, 2010). Mutants defective in BB or heme utilization demonstrate little to no effect on virulence(Cendrowski *et al.*, 2004; Gat *et al.*, 2008; Carlson *et al.*, 2009). What makes PB more relevant to *B. anthracis* pathogenesis? We attribute it to regulation and structural features that enable avoidance of the innate immune response and increased iron acquisition.

Studies of PB regulation indicate that conditions relevant to host physiology (5% CO_2 and 37°C) increase PB production but decrease BB production(Garner *et al.*, 2004; Koppisch *et al.*, 2005; Wilson *et al.*, 2010). The differences in PB and BB regulation reflect what is known about the contribution of PB to iron acquisition in the mammalian host over BB. In addition to iron sequestration, neutrophils produce a protein known as siderocalin or lipocalin(Abergel, Clifton, *et al.*, 2008). Siderocalin directly interferes with pathogen iron acquisition by binding siderophores(Abergel, Clifton, *et al.*, 2008). It is capable of binding to ferric-enterobactin and ferric-BB but not glycosylated enterobactin (salmochelin), as glycosylation makes it too large for the binding pocket(Abergel *et al.*, 2006). Ferric-PB is the correct size and charge to be bound by siderocalin(Abergel *et al.*, 2006). However, siderocalin did not recognize PB in *in vitro* studies leading to its designation as the anthrax "stealth siderophore"(Abergel *et al.*, 2006). Abergel, *et. al.* predicted the orientation of the 3,4-DHB moieties creates a steric hindrance, thus preventing interaction with the rigid binding pocket of siderocalin(Abergel *et al.*, 2006). Another interesting feature of the 3,4-DHB moieties is that they appear to improve sequestration of ferric iron

away from transferrin(Abergel, Zawadzka, *et al.*, 2008). While enterobactin has a higher overall affinity for ferric iron, PB removes Fe^{3+} from transferrin up to 6 times more rapidly than enterobactin and 100 times more quickly than the hydroxamate/α-hydroxycarboxylate aerobactin(Abergel, Zawadzka, *et al.*, 2008). The authors hypothesized the 3,4-DHB moieties were responsible for this phenomenon. The catechol moieties improve affinity for iron over hydroxamate moieties, hence the increased rate compared to aerobactin(Abergel, Zawadzka, *et al.*, 2008). Since the overall affinity of PB is still lower than enterobactin, perhaps the unique orientation of the hydroxyl groups provide an increased rate of transfer(Abergel, Zawadzka, *et al.*, 2008). Avoiding sequestration by siderocalin, and thus detection of the innate immune response, together with an increased ability to retrieve ferric iron from transferrin help account for PB's relevance in *B. anthracis* pathogenesis.

A Target for Antibiotics?:

The unique structure of PB confers multiple advantages within the mammalian host environment, and this along with the patterns of regulation, support extrapolation of murine data to the human host. As is the case with other siderophore-producing pathogens, such as *Mycobacterium tuberculosis*, this implies PB use (inclusive of biosynthesis, transport and iron removal) is a viable target for rational anti-*anthracis* drug design(Ferreras *et al.*, 2005). To date, two studies have reported the generation or identification of small molecules targeting PB biosynthetic machinery. First, a rationally-designed acylsulfate analogue of 3,4-DHB-AMP can compete for 3,4-DHB binding to AsbC with submicro-molar affinities(Pfleger *et al.*, 2007). More recently, two small molecules termed baulamycin A and baulamycin B, were found to be potent inhibitors of AsbA activity *in vitro* and of *B. anthracis* growth in both IDM and IRM(Tripathi *et al.*, 2014). These compounds have yet to be tested in animal models. Regardless, the requirement of PB for virulence in *B. anthracis*, and for siderophores in other pathogens, warrants further exploration of small molecules that can inhibit siderophore production and/or use. In

addition, the possibility of exploiting this necessity through the generation of siderophore-drug conjugates is an intriguing prospect in the quest for new antibiotics.

Summary and Future Directions:

This review summarized the current knowledge about PB in the context of the pathogen, *Bacillus anthracis*. Interestingly, recent studies have revealed many features of PB regulation, biosynthesis, structure and transport that are unusual, or even unique, in the field of bacterial siderophores. Together, these features enable *B. anthracis* to produce a siderophore under relevant host conditions, that not only gathers the requisite iron for growth, but efficiently and all while "flying under the radar" of host innate immunity. However, many gaps remain in the current body of knowledge about PB. These include identification of the mechanisms responsible for apo-PB export, iron-removal from holo-PB and regulation of PB biosynthesis. Future research into PB use by *B. anthracis* should focus on addressing these issues and may reveal other non-canonical methods for siderophore acquisition systems. In addition to broadening the field of siderophore research, understanding the "life cycle" of PB use by *B. anthracis* is key for the continued development of targeted antimicrobial therapies.

Figure Legends:

Figure 1. Structure and biosynthesis of petrobactin by Bacillus anthracis. **A**) Following generation of 3,4-DHB by AsbF (red), it is incorporated into petrobactin by three NRPS enzymes, AsbCDE (black text). First it is loaded on to the aryl-carrier protein AsbD by the transferase AsbC. Condensation of 3,4-DHB to a spermidine arm is performed by AsbE. Two isomers are formed, though only the isomer containing 3,4-DHB at the N1-terminus is incorporated into the final product. **B**) NIS enzymes AsbAB (blue text) condense the citrate backbone to spermidine arms. AsbA efficiently catalyzes the initial reaction of a single spermidine and citrate while AsbB condenses spermidine to a molecule of citryl-spermidine or 3,4-DHB-citryl-spermidine. AsbE and AsbD cap the backbone with 3,4-DHB moieties. **C**) Structure of petrobactin. A citrate backbone (blue) with two spermidine arms (green) each capped with a 3,4-DHB moiety (black). A single molecule of ferric iron is coordinated between each of the 3,4-DHB catechol moieties and the α-hydroxycarboxylate of the citrate backbone (red)(Nusca *et al.*, 2012).

Figure 2. AsbF structure and active site. **A**) Crystal structure of AsbF. The eight β-sheet TIM-barrel (green) occludes the N-terminus (blue) while the C-terminus (salmon, arrow) is exposed. A helical loop (yellow) caps the barrel, closing the active site. **B**) AsbF structure rotated to demonstrate the active site. The Mn2+ is coordinated between residues found within the barrel (black) and 3,4-DHB. In turn, the 3,4-DHB is coordinated by the aromatic residues (red) contributed by helical loops(Guex and Peitsch, 1997; Pfleger *et al.*, 2008).

Figure 3. AsbB structure and active site. **A**) Structure and active site of monomeric AsbB. It is composed of three domains; the thumb (yellow), the palm (blue) and the finger (green). The active site is positioned between the palm and finger domains. Basic residues in the palm (red) are predicted to bind ATP/ADP while acidic residues in the finger domain (black, purple) stabilize and selectively recruit spermidine to the active site. **B**) AsbB dimerization is coordinated by the thumb domain (yellow) of one protein with the finger domain (green) of the second (top; view from bottom). This creates a solvent exposed channel (bottom; side view)(Guex and Peitsch, 1997; Nusca *et al.*, 2012).

Figure 4. Proposed schematic of petrobactin import, export and iron removal in B. anthracis. Petrobactin (PB, yellow star) is exported via an unknown mechanism. In the supernatant, PB chelates ferric iron and is bound for import by the cell surface recognition protein FpuA (orange). The Fe-PB is then transported by either of two permeases (blue) FpuB or FatCD complexed with an ATPase (green). Energy for transport via FpuB is provided by either FpuC or FpuD while FatCD complexes with the ATPase FatE., The iron is removed from PB by an unknown mechanism (gray) resulting in reduction of iron from intact or hydrolyzed PB(Carlson *et al.*, 2010; Dixon *et al.*, 2012).

Works Cited:

Abergel, R.J., Clifton, M.C., Pizarro, J.C., Warner, J. a, Shuh, D.K., Strong, R.K., and Raymond, K.N. (2008) The siderocalin/enterobactin interaction: A link between mammalian immunity and bacterial iron transport. *J Am Chem Soc* **130**: 11524–34.

Abergel, R.J., Wilson, M.K., Arceneaux, J.E.L., Hoette, T.M., Strong, R.K., Byers, B.R., and Raymond, K.N. (2006) Anthrax pathogen evades the mammalian immune system through stealth siderophore production. *Proc Natl Acad Sci U S A* **103**: 18499–18503.

Abergel, R.J., Zawadzka, A.M., and Raymond, K.N. (2008) Petrobactin-mediated iron transport in pathogenic bacteria: Coordination chemistry of an unusual 3,4-catecholate/citrate siderophore. *J Am Chem Soc* **130**: 2124–2125.

Bagg, A., and Neilands, J. (1987) Ferric uptake regulation protein acts as a repressor, employing iron (II) as a cofactor to bind the operator of an iron transport operon in Escherichia coli. *Biochemistry* **26**: 5471–5477.

Banks, D.J., Barnajian, M., Maldonado-Arocho, F.J., Sanchez, A.M., and Bradley, K.A. (2005) Anthrax toxin receptor 2 mediates Bacillus anthracis killing of macrophages following spore challenge. *Cell Microbiol* **7**: 1173–1185.

Barbeau, K., Zhang, G., Live, D.H., and Butler, A. (2002) Petrobactin, a photoreactive siderophore produced by the oil-degrading marine bacterium Marinobacter hydrocarbonoclasticus. *J Am Chem Soc* **124**: 378–9.

Braun, V., and Hantke, K. (2011) Recent insights into iron import by bacteria. *Curr Opin Chem Biol* **15**: 328–34.

Brittingham, K.C., Ruthel, G., Panchal, R.G., Fuller, C.L., Ribot, W.J., Hoover, T.A., *et al.* (2005) Dendritic cells endocytose Bacillus anthracis spores: Implications for anthrax pathogenesis. *J Immunol* **174**: 5545–5552.

Carlson, P.E., Bourgis, A.E.T., Hagan, A.K., and Hanna, P.C. (2015) Global gene expression by Bacillus anthracis during growth in mammalian blood. *Pathog Dis* **73**: ftv061.

Carlson, P.E., Carr, K. a, Janes, B.K., Anderson, E.C., and Hanna, P.C. (2009) Transcriptional profiling of Bacillus anthracis Sterne (34F2) during iron starvation. *PLoS One* **4**: e6988.

Carlson, P.E., Dixon, S.D., and Hanna, P.C. (2013) Anthrax and iron. In *Regulation of Bacterial Virulence*. Vasil, M.L., and Darwin, A.J. (eds). ASM Press, Washington, DC. pp. 307–314.

Carlson, P.E., Dixon, S.D., Janes, B.K., Carr, K. a, Nusca, T.D., Anderson, E.C., *et al.* (2010) Genetic analysis of petrobactin transport in Bacillus anthracis. *Mol Microbiol* **75**: 900–9.

Cendrowski, S., MacArthur, W., and Hanna, P. (2004) Bacillus anthracis requires siderophore biosynthesis for growth in macrophages and mouse virulence. *Mol Microbiol* **51**: 407–17.

Challis, G.L. (2005) A widely distributed bacterial pathway for siderophore biosynthesis independent of nonribosomal peptide synthetases. *ChemBioChem* **6**: 601–611.

Chazarreta-Cifre, L., Martiarena, L., Mendoza, D. de, and Altabe, S.G. (2011) Role of ferredoxin and flavodoxins in Bacillus subtilis fatty acid desaturation. *J Bacteriol* **193**: 4043–8.

Conti, E., Stachelhaus, T., Marahiel, M., and Brick, P. (1997) Structural basis for the activation of phenylalanine in the non-ribosomal biosynthesis of gramicidin S. *EMBO J* **16**: 4174–4183.

Cote, C.K., Welkos, S.L., and Bozue, J. (2011) Key aspects of the molecular and cellular basis of

inhalational anthrax. *Microbes Infect* **13**: 1146–1155.

Dixon, S.D., Janes, B.K., Bourgis, A., Carlson, P.E., and Hanna, P.C. (2012) Multiple ABC transporters are involved in the acquisition of petrobactin in Bacillus anthracis. *Mol Microbiol* **84**: 370–82.

Dixon, T.C., Meselson, M., Guillemin, J., and Hanna, P.C. (1999) Anthrax. *N Engl J Med* **341**: 815–826.

Ernst, J., Bennett, R., and Rothfield, L. (1978) Constitutive expression of the iron-enterochelin and ferrichrome uptake systems in a mutant strain of Salmonella typhimurium. *J Bacteriol* **135**: 928–934.

Ferreras, J.A., Ryu, J.S., Lello, F. Di, Tan, D.S., and Quadri, L.E.N. (2005) Small-molecule inhibition of siderophore biosynthesis in Mycobacterium tuberculosis and Yersinia pestis. *Nat Chem Biol* **1**: 29–32.

Finkelstein, R.A., Sciortino, C. V, and McIntosh, M.A. (1983) Role of iron in microbe-host interactions. *Rev Infect Dis* **5 Suppl 4**: S759–S777.

Finking, R., and Marahiel, M. (2004) Biosynthesis of nonribosomal peptides. *Annu Rev Microbiol* **58**: 453–488.

Fox, D.T., Hotta, K., Kim, C.Y., and Koppisch, A.T. (2008) The missing link in petrobactin biosynthesis: asbF encodes a (-)-3-dehydroshikimate dehydratase. *Biochemistry* **47**: 12251–12253.

Friedlander, A., Welkos, S., Pitt, M., Ezzell, J., Worsham, P., Rose, K., *et al.* (1993) Postexposure prophylaxis against experimental inhalation anthrax. *J Infect Dis* **167**: 1239–1242.

Ganz, T. (2013) Systemic iron homeostasis. *Physiol Rev* **93**: 1721–41.

Gardner, R.A., Kinkade, R., Wang, C., and Phanstiel, O. (2004) Total synthesis of petrobactin and its homologues as potential growth stimuli for Marinobacter hydrocarbonoclasticus, an oil-degrading bacteria. *J Org Chem* **69**: 3530–7.

Garner, B.L., Arceneaux, J.E.L., and Byers, B.R. (2004) Temperature control of a 3,4-dihydroxybenzoate (protocatechuate)-based siderophore in Bacillus anthracis. *Curr Microbiol* **49**: 89–94.

Gat, O., Zaide, G., Inbar, I., Grosfeld, H., Chitlaru, T., Levy, H., and Shafferman, A. (2008) Characterization of Bacillus anthracis iron-regulated surface determinant (Isd) proteins containing NEAT domains. *Mol Microbiol* **70**: 983–99.

Guex, N., and Peitsch, M.C. (1997) SWISS-MODEL and the Swiss-PdbViewer: An environment for comparative protein modeling. *Electrophoresis* **18**: 2714–2723.

Hantke, K. (1981) Regulation of ferric iron transport in Escherichia coli K12: Isolation of a constitutive mutant. *Mol Gen Genet* **182**: 288–292.

Hider, R.C., and Kong, X. (2010) Chemistry and biology of siderophores. *Nat Prod Rep* **27**: 637–57.

Homann, V. V, Edwards, K.J., Webb, E. a, and Butler, A. (2009) Siderophores of Marinobacter aquaeolei: Petrobactin and its sulfonated derivatives. *Biometals* **22**: 565–71.

Hotta, K., Kim, C.-Y., Fox, D.T., and Koppisch, A.T. (2010) Siderophore-mediated iron acquisition in Bacillus anthracis and related strains. *Microbiology* **156**: 1918–25.

Kadi, N., Oves-Costales, D., Barona-Gomez, F., and Challis, G.L. (2007) A new family of ATP-dependent oligomerization-macrocyclization biocatalysts. *Nat Chem Biol* **3**: 652–656.

Keating, T., Marshall, C., and Walsh, C. (2000) Reconstitution and characterization of the Vibrio cholerae vibriobactin synthetase from VibB, VibE, VibF, and VibH. *Biochemistry* **39**: 15522–15530.

Keating, T., Marshall, C., Walsh, C., and Keating, A. (2002) The structure of VibH represents nonribosomal peptide synthetase condensation, cyclization and epimerization domains. *Nat Struct Biol*

9: 522–526.

Koppisch, A.T., Browder, C.C., Moe, A.L., Shelley, J.T., Kinkel, B. a, Hersman, L.E., *et al.* (2005) Petrobactin is the primary siderophore synthesized by Bacillus anthracis str. Sterne under conditions of iron starvation. *Biometals* **18**: 577–85.

Koppisch, A.T., Dhungana, S., Hill, K.K., Boukhalfa, H., Heine, H.S., Colip, L. a, *et al.* (2008) Petrobactin is produced by both pathogenic and non-pathogenic isolates of the Bacillus cereus group of bacteria. *Biometals* **21**: 581–9.

Langman, L., Young, I.G., Frost, G.E., Rosenberg, H., and Gibson, F. (1972) Enterochelin system of iron transport in Escherichia coli: Mutations affecting ferric-enterochelin esterase. *J Bacteriol* **112**: 1142–1149.

Lavrrar, J., and Mcintosh, M. (2003) Architecture of a Fur binding site: A comparative analysis. *J Bacteriol* **185**: 2194–2202.

Lee, J.Y., Janes, B.K., Passalacqua, K.D., Pfleger, B.F., Bergman, N.H., Liu, H., *et al.* (2007) Biosynthetic analysis of the petrobactin siderophore pathway from Bacillus anthracis. *J Bacteriol* **189**: 1698–710.

Lee, J.Y., Passalacqua, K.D., Hanna, P.C., and Sherman, D.H. (2011) Regulation of petrobactin and bacillibactin biosynthesis in Bacillus anthracis under iron and oxygen variation. *PLoS One* **6**: e20777.

Lincoln, R., Walker, J., Klein, F., Rosenwald, A., and Jones, W.J. (1967) Technical manuscript 349: Value of field data for extrapolation in anthrax. .

May, J.J., Kessler, N., Marahiel, M. a, and Stubbs, M.T. (2002) Crystal structure of DhbE, an archetype for aryl acid activating domains of modular nonribosomal peptide synthetases. *Proc Natl Acad Sci U S A* **99**: 12120–5.

Miethke, M. (2013) Molecular strategies of microbial iron assimilation: from high-affinity complexes to cofactor assembly systems. *Met Integr biometal Sci* **5**: 15–28.

Miethke, M., and Marahiel, M. a (2007) Siderophore-based iron acquisition and pathogen control. *Microbiol Mol Biol Rev* **71**: 413–451.

Müller, K., Matzanke, B.F., Schünemann, V., Trautwein, a X., and Hantke, K. (1998) FhuF, an iron-regulated protein of Escherichia coli with a new type of [2Fe-2S] center. *Eur J Biochem* **258**: 1001–8.

Nusca, T.D. (2012) Detailed analysis of biosynthetic components for the virulence-associated siderophore petrobactin from Bacillus anthracis. .

Nusca, T.D., Kim, Y., Maltseva, N., Lee, J.Y., Eschenfeldt, W., Stols, L., *et al.* (2012) Functional and structural analysis of the siderophore synthetase AsbB through reconstitution of the petrobactin biosynthetic pathway from Bacillus anthracis. *J Biol Chem* **287**: 16058–72.

Oves-Costales, D., Kadi, N., and Challis, G.L. (2009) The long-overlooked enzymology of a nonribosomal peptide synthetase-independent pathway for virulence-conferring siderophore biosynthesis. *Chem Commun* 6530–41.

Oves-Costales, D., Kadi, N., Fogg, M.J., Song, L., Wilson, K.S., and Challis, G.L. (2007) Enzymatic logic of anthrax stealth siderophore biosynthesis: AsbA catalyzes ATP-dependent condensation of citric acid and spermidine. *J Am Chem Soc* **129**: 8416–8417.

Oves-Costales, D., Kadi, N., Fogg, M.J., Song, L., Wilson, K.S., and Challis, G.L. (2008) Petrobactin biosynthesis: AsbB catalyzes condensation of spermidine with N8-citryl-spermidine and its N1-(3,4-dihydroxybenzoyl) derivative. *Chem Commun* 4034–6.

Oves-Costales, D., Song, L., and Challis, G.L. (2009) Enantioselective desymmetrisation of citric acid catalysed by the substrate-tolerant petrobactin biosynthetic enzyme AsbA. *Chem Commun* 1389–91.

Palmateer, N.E., Hope, V.D., Roy, K., Marongiu, A., White, J.M., Grant, K. a, *et al.* (2013) Infections with spore-forming bacteria in persons who inject drugs, 2000-2009. *Emerg Infect Dis* **19**: 29–34.

Passalacqua, K.D., Bergman, N.H., Lee, J.Y., Sherman, D.H., and Hanna, P.C. (2007) The global transcriptional responses of Bacillus anthracis Sterne (34F2) and a Delta sodA1 mutant to paraquat reveal metal ion homeostasis imbalances during endogenous superoxide stress. *J Bacteriol* **189**: 3996–4013.

Pfleger, B.F., Kim, Y., Nusca, T.D., Maltseva, N., Lee, J.Y., Rath, C.M., *et al.* (2008) Structural and functional analysis of AsbF: Origin of the stealth 3,4-dihydroxybenzoic acid subunit for petrobactin biosynthesis. *Proc Natl Acad Sci U S A* **105**: 17133–8.

Pfleger, B.F., Lee, J.Y., Somu, R. V, Aldrich, C.C., Hanna, P.C., and Sherman, D.H. (2007) Characterization and analysis of early enzymes for petrobactin biosynthesis in Bacillus anthracis. *Biochemistry* **46**: 4147–57.

Pohl, S., Tu, W.Y., Aldridge, P.D., Gillespie, C., Hahne, H., Mäder, U., *et al.* (2011) Combined proteomic and transcriptomic analysis of the response of Bacillus anthracis to oxidative stress. *Proteomics* **11**: 3036–55.

Ross, J.M. (1957) The pathogenesis of anthrax following the administration of spores by the respiratory route. *J Pathol Bacteriol* **73**: 485–494.

Saha, R., Saha, N., Donofrio, R.S., and Bestervelt, L.L. (2013) Microbial siderophores: A mini review. *J Basic Microbiol* **53**: 303–17.

Schmelz, S., Kadi, N., McMahon, S.A., Song, L., Oves-Costales, D., Oke, M., *et al.* (2009) AcsD catalyzes enantioselective citrate desymmetrization in siderophore biosynthesis. *Nat Chem Biol* **5**: 174–82.

Schneider, A., and Marahiel, M. (1998) Genetic evidence for a role of thioesterase domains, integrated in or associated with peptide synthetases, in non-ribosomal peptide biosynthesis in Bacillus subtilis. *Arch Microbiol* **169**: 404–410.

Sieber, S., and Marahiel, M. (2008) Learning from nature's drug factories: Nonribosomal synthesis of macrocyclic peptides. *J Bacteriol* **185**: 7036–7043.

Sierro, N., Makita, Y., Hoon, M. de, and Nakai, K. (2008) DBTBS: A database of transcriptional regulation in Bacillus subtilis containing upstream intergenic conservation information. *Nucleic Acids Res* **36**: D93–6.

Stachelhaus, T., Mootz, H., and Marahiel, M. (1999) The specificity-conferring code of adenylation domains in nonribosomal peptide synthetases. *Chem Biol* **6**: 493–505.

Stojiljkovic, I., Baumler, A., and Hantke, K. (1994) Idientification and characterization of new iron-regulated Escherichia coli genes by a Fur titration assay. *J Mol Biol* **236**: 531–545.

Tripathi, A., Schofield, M.M., Chlipala, G.E., Schultz, P.J., Yim, I., Newmister, S.A., *et al.* (2014) Baulamycins A and B, broad-spectrum antibiotics identified as inhibitors of siderophore siosynthesis in Staphylococcus aureus and Bacillus anthracis. *J Am Chem Soc* **136**: 1579–1586.

Tu, W.Y., Pohl, S., Gray, J., Robinson, N.J., Harwood, C.R., and Waldron, K.J. (2012) Cellular iron distribution in Bacillus anthracis. *J Bacteriol* **194**: 932–40.

Wandersman, C., and Delepelaire, P. (2004) Bacterial iron sources: From siderophores to hemophores. *Annu Rev Microbiol* **58**: 611–47.

Weber, T., Baumgartner, R., Renner, C., Marahiel, M., and Holak, T. (2000) Solution structure of PCP, a prototype for the peptidyl carrier domains of modular peptide synthetases. *Structure* **8**: 407–418.

Wilson, M.K., Abergel, R.J., Arceneaux, J.E.L., Raymond, K.N., and Byers, B.R. (2010) Temporal production of the two Bacillus anthracis siderophores, petrobactin and bacillibactin. *Biometals* **23**: 129–34.

Yeterian, E., Martin, L.W., Guillon, L., Journet, L., Lamont, I.L., and Schalk, I.J. (2010) Synthesis of the siderophore pyoverdine in Pseudomonas aeruginosa involves a periplasmic maturation. *Amino Acids* **38**: 1447–59.

Yeterian, E., Martin, L.W., Lamont, I.L., and Schalk, I.J. (2010) An efflux pump is required for siderophore recycling by Pseudomonas aeruginosa. *Environ Microbiol Rep* **2**: 412–8.

Zhang, G., Amin, S.A., Küpper, F.C., Holt, P.D., Carrano, C.J., and Butler, A. (2009) Ferric stability constants of representative marine siderophores: Marinobactins, aquachelins, and petrobactin. *Inorg Chem* **48**: 11466–73.

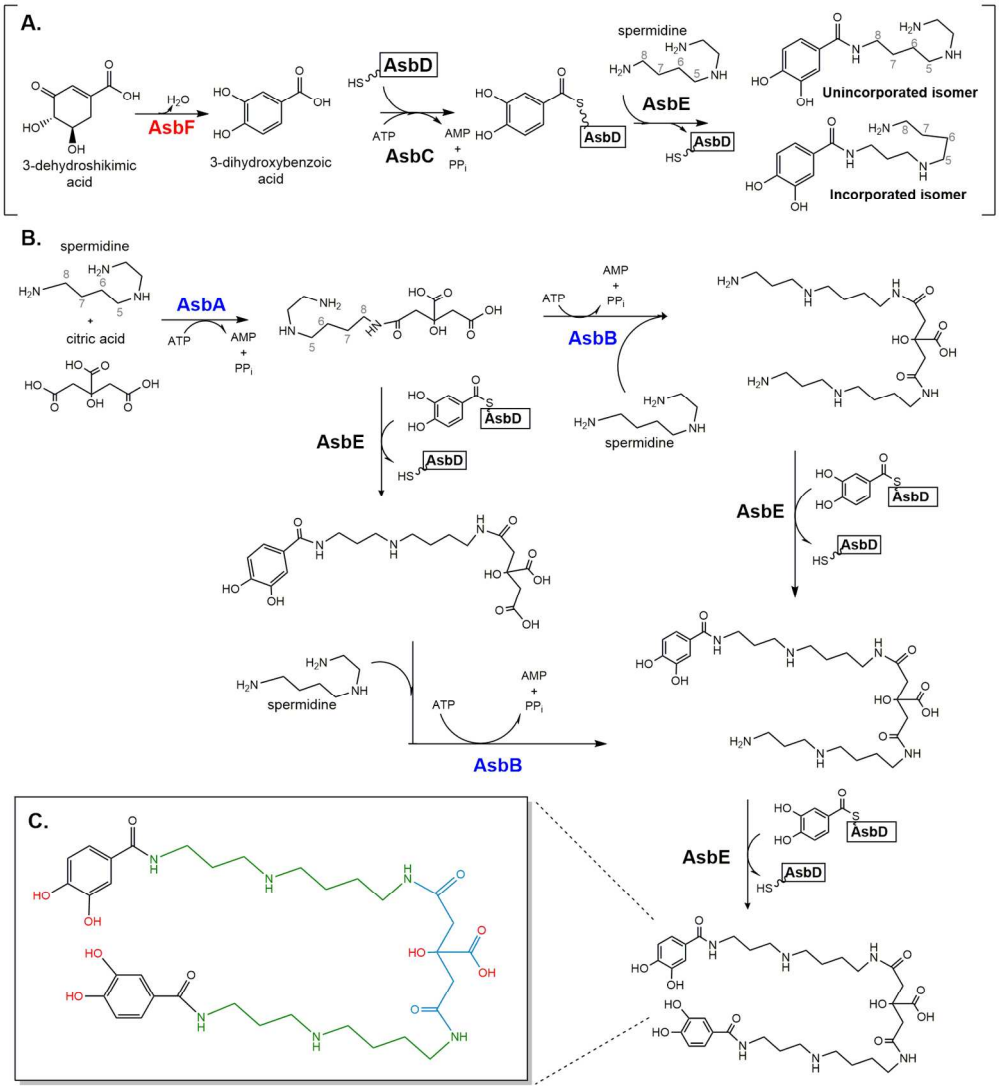

Figure 1. Structure and biosynthesis of petrobactin by Bacillus anthracis. A) Following generation of 3,4-DHB by AsbF (red), it is incorporated into petrobactin by three NRPS enzymes, AsbCDE (black text). First it is loaded on to the aryl-carrier protein AsbD by the transferase AsbC. Condensation of 3,4-DHB to a spermidine arm is performed by AsbE. Two isomers are formed, though only the isomer containing 3,4-DHB at the N1-terminus is incorporated into the final product. B) NIS enzymes AsbAB (blue text) condense the citrate backbone to spermidine arms. AsbA efficiently catalyzes the initial reaction of a single spermidine and citrate while AsbB condenses spermidine to a molecule of citryl-spermidine or 3,4-DHB-citryl-spermidine. AsbE and AsbD cap the backbone with 3,4-DHB moieties. C) Structure of petrobactin. A citrate backbone (blue) with two spermidine arms (green) each capped with a 3,4-DHB moiety (black). A single molecule of ferric iron is coordinated between each of the 3,4-DHB catechol moieties and the α-hydroxycarboxylate of the citrate backbone (red)(Nusca et al., 2012).

150x163mm (300 x 300 DPI)

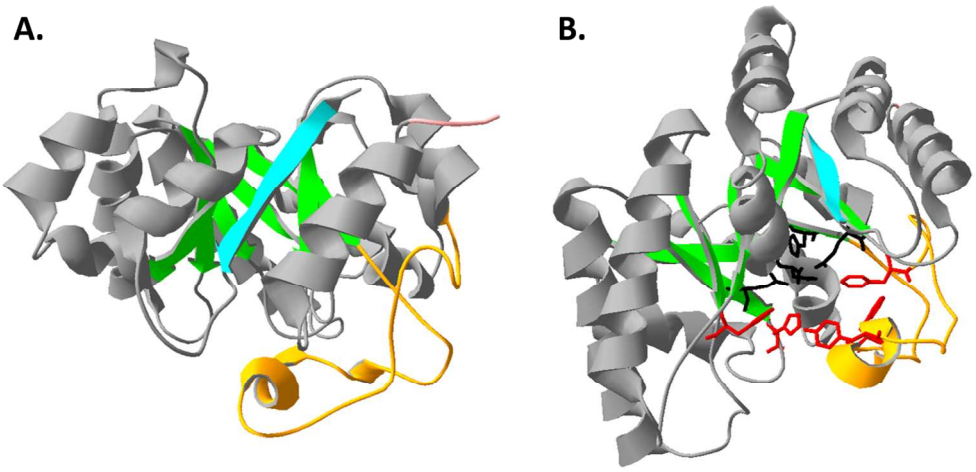

Figure 2. AsbF structure and active site. A) Crystal structure of AsbF. The eight β-sheet TIM-barrel (green) occludes the N-terminus (blue) while the C-terminus (salmon, arrow) is exposed. A helical loop (yellow) caps the barrel, closing the active site. B) AsbF structure rotated to demonstrate the active site. The Mn2+ is coordinated between residues found within the barrel (black) and 3,4-DHB. In turn, the 3,4-DHB is coordinated by the aromatic residues (red) contributed by helical loops(Guex and Peitsch, 1997; Pfleger et al., 2008).

373x183mm (96 x 96 DPI)

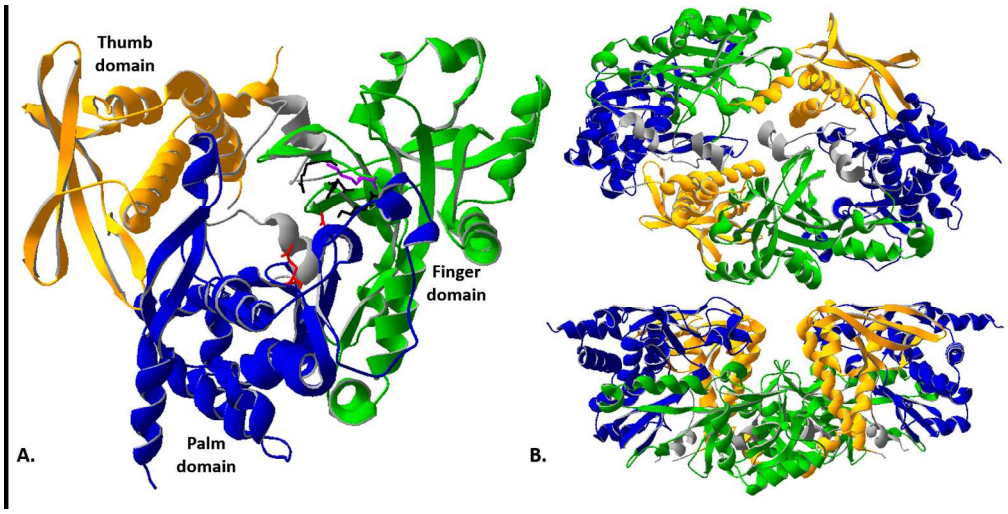

Figure 3. AsbB structure and active site. A) Structure and active site of monomeric AsbB. It is composed of three domains; the thumb (yellow), the palm (blue) and the finger (green). The active site is positioned between the palm and finger domains. Basic residues in the palm (red) are predicted to bind ATP/ADP while acidic residues in the finger domain (black, purple) stabilize and selectively recruit spermidine to the active site. B) AsbB dimerization is coordinated by the thumb domain (yellow) of one protein with the finger domain (green) of the second (top; view from bottom). This creates a solvent exposed channel (bottom; side view)(Guex and Peitsch, 1997; Nusca et al., 2012).

465x233mm (96 x 96 DPI)

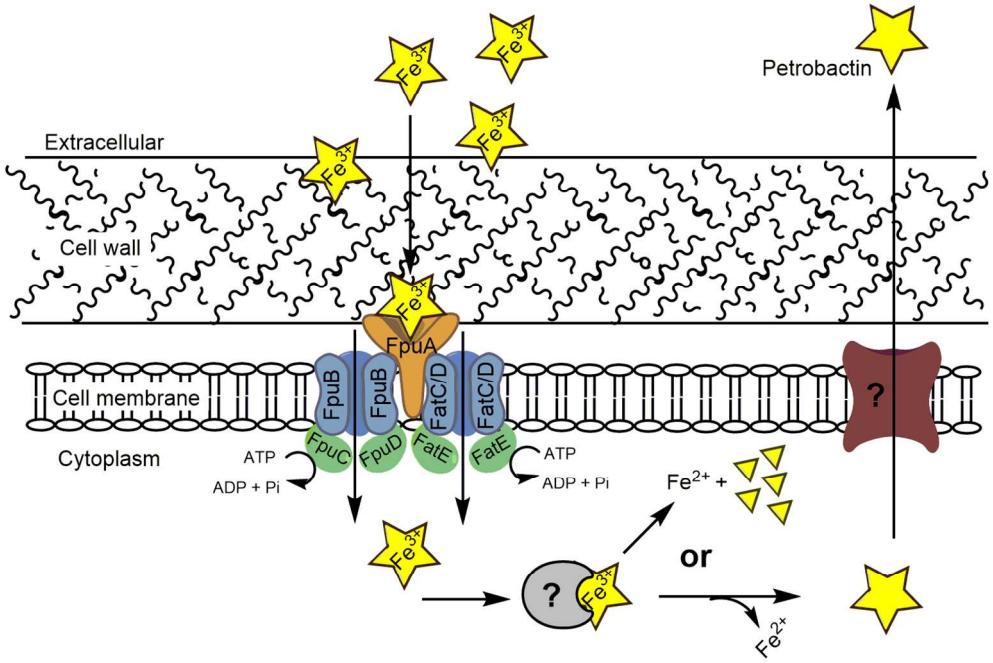

Figure 4. Proposed schematic of petrobactin import, export and iron removal in B. anthracis. Petrobactin (PB, yellow star) is exported via an unknown mechanism. In the supernatant, PB chelates ferric iron and is bound for import by the cell surface recognition protein FpuA (orange). The Fe-PB is then transported by either of two permeases (blue) FpuB or FatCD complexed with an ATPase (green). Energy for transport via FpuB is provided by either FpuC or FpuD while FatCD complexes with the ATPase FatE., The iron is removed from PB by an unknown mechanism (gray) resulting in reduction of iron from intact or hydrolyzed PB(Carlson et al., 2010; Dixon et al., 2012).

129x86mm (300 x 300 DPI)

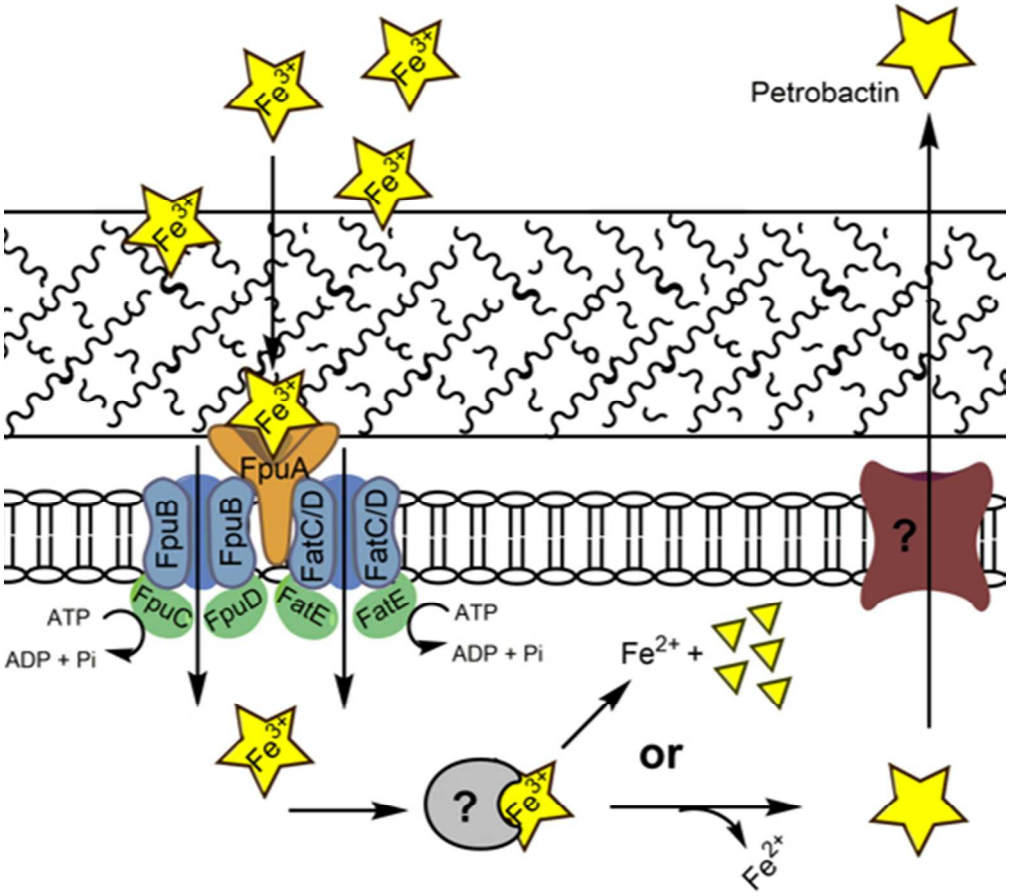

Alternative Figure 4 in eTOC thumbnail format - IF NEEDED FOR WEBSITE IMAGE

149x135mm (96 x 96 DPI)